JCI The Journal of Clinical Investigation

Insulin demand regulates β cell number via the unfolded protein response

Rohit B. Sharma, … , Peter Arvan, Laura C. Alonso

J Clin Invest. 2015;125(10):3831-3846. https://doi.org/10.1172/JCI79264.

Research Article **Endocrinology**

Although stem cell populations mediate regeneration of rapid turnover tissues, such as skin, blood, and gut, a stem cell reservoir has not been identified for some slower turnover tissues, such as the pancreatic islet. Despite lacking identifiable stem cells, murine pancreatic β cell number expands in response to an increase in insulin demand. Lineage tracing shows that new β cells are generated from proliferation of mature, differentiated β cells; however, the mechanism by which these mature cells sense systemic insulin demand and initiate a proliferative response remains unknown. Here, we identified the β cell unfolded protein response (UPR), which senses insulin production, as a regulator of β cell proliferation. Using genetic and physiologic models, we determined that among the population of β cells, those with an active UPR are more likely to proliferate. Moreover, subthreshold endoplasmic reticulum stress (ER stress) drove insulin demand–induced β cell proliferation, through activation of ATF6. We also confirmed that the UPR regulates proliferation of human β cells, suggesting that therapeutic UPR modulation has potential to expand β cell mass in people at risk for diabetes. Together, this work defines a stem cell–independent model of tissue homeostasis, in which differentiated secretory cells use the UPR sensor to adapt organ size to meet demand.

Insulin demand regulates β cell number via the unfolded protein response

Rohit B. Sharma,[1] Amy C. O'Donnell,[2] Rachel E. Stamateris,[1] Binh Ha,[1] Karen M. McCloskey,[2] Paul R. Reynolds,[3] Peter Arvan,[4] and Laura C. Alonso[1]

[1]Diabetes Division, Department of Medicine, University of Massachusetts (UMass) Medical School, Worcester, Massachusetts, USA. [2]University of Pittsburgh School of Medicine, Pittsburgh, Pennsylvania, USA. [3]Department of Pediatrics, National Jewish Health, Denver, Colorado, USA. [4]Metabolism, Endocrinology, and Diabetes, University of Michigan, Ann Arbor, Michigan, USA.

Although stem cell populations mediate regeneration of rapid turnover tissues, such as skin, blood, and gut, a stem cell reservoir has not been identified for some slower turnover tissues, such as the pancreatic islet. Despite lacking identifiable stem cells, murine pancreatic β cell number expands in response to an increase in insulin demand. Lineage tracing shows that new β cells are generated from proliferation of mature, differentiated β cells; however, the mechanism by which these mature cells sense systemic insulin demand and initiate a proliferative response remains unknown. Here, we identified the β cell unfolded protein response (UPR), which senses insulin production, as a regulator of β cell proliferation. Using genetic and physiologic models, we determined that among the population of β cells, those with an active UPR are more likely to proliferate. Moreover, subthreshold endoplasmic reticulum stress (ER stress) drove insulin demand–induced β cell proliferation, through activation of ATF6. We also confirmed that the UPR regulates proliferation of human β cells, suggesting that therapeutic UPR modulation has potential to expand β cell mass in people at risk for diabetes. Together, this work defines a stem cell–independent model of tissue homeostasis, in which differentiated secretory cells use the UPR sensor to adapt organ size to meet demand.

Introduction

Diabetes occurs when pancreatic β cells fail to meet insulin demand, due to loss of β cell mass and function (1, 2). In the end-stage spiral that leads to diabetes, β cell mass and function are linked via decompensated endoplasmic reticulum stress (ER stress). Severely overworked β cells are more likely to die, leading to loss of β cell mass; β cell loss increases stress on remaining β cells, impairing their function (3–7). For both type 1 and type 2 diabetes, an important therapeutic goal is to find tools to regenerate β cells, so as to restore endogenous insulin production capacity.

Some strains of mice robustly increase β cell number in response to increased insulin demand (8). No local stem cell population has been found in islets, nor do hematogenous stem cells participate in β cell expansion (9). Lineage-tracing studies show that the primary means of generating new β cells in adult mice is proliferation of fully differentiated, mature β cells (10, 11). In fact, all β cells are reported to have equal potency to generate new β cells, implying a different model of tissue homeostasis in which the proliferative reservoir consists of fully differentiated cells (12, 13). Since the rate of β cell proliferation is strongly influenced by the metabolic environment of the host (14–16), in some cases trumping islet-intrinsic factors (17, 18), the working model in the field has been that circulating factors regulate β cell proliferation. Many different signals have been proposed to drive β cell proliferation in response to insulin demand, principally nutrients (14, 15, 19, 20) and growth factors (8, 21–23). However, no circulating signal explains all the observations, and models in which a distant organ senses insulin demand and directs β cells to proliferate are complicated and indirect.

Here, we present evidence supporting a simpler hypothesis: that the β cell itself senses unmet insulin demand via activation of unfolded protein response (UPR) secretory peptide synthesis sensors, which trigger a proliferative response. When demand increases, it is well established that β cells increase proinsulin synthesis, activating the UPR (3, 7). We find that β cells with active UPR are more likely to proliferate, that engaging mild additional ER stress increases proliferation in the context of high glucose, and that UPR activation is required for driving proliferation in several different models. We trace the proliferative signal to the ATF6 pathway and verify that UPR also regulates proliferation in human β cells (all instances of Atf6 refer to Atf6α). Taken together, these findings outline a mechanism by which insulin demand regulates β cell number and suggest a model of tissue homeostasis, independent of stem cells, in which secretory cells use the UPR mechanism to sense demand and increase cell number when demand exceeds capacity.

Results

Proteomics screen to identify in vivo drivers of β cell proliferation reveals activation of the UPR without decompensation. Hyperglycemia increases insulin demand. In mice, modestly raising blood glucose by direct i.v. glucose infusion increases β cell proliferation (15, 24, 25). To identify new pathways driving β cell proliferation, islets were isolated after a 4-day exposure to either normal or elevated blood glucose (Supplemental Figure 1; supplemental material

Conflict of interest: The authors have declared that no conflict of interest exists.
Submitted: October 10, 2014; **Accepted:** August 13, 2015.
Reference information: *J Clin Invest*. 2015;125(10):3831–3846. doi:10.1172/JCI79264.

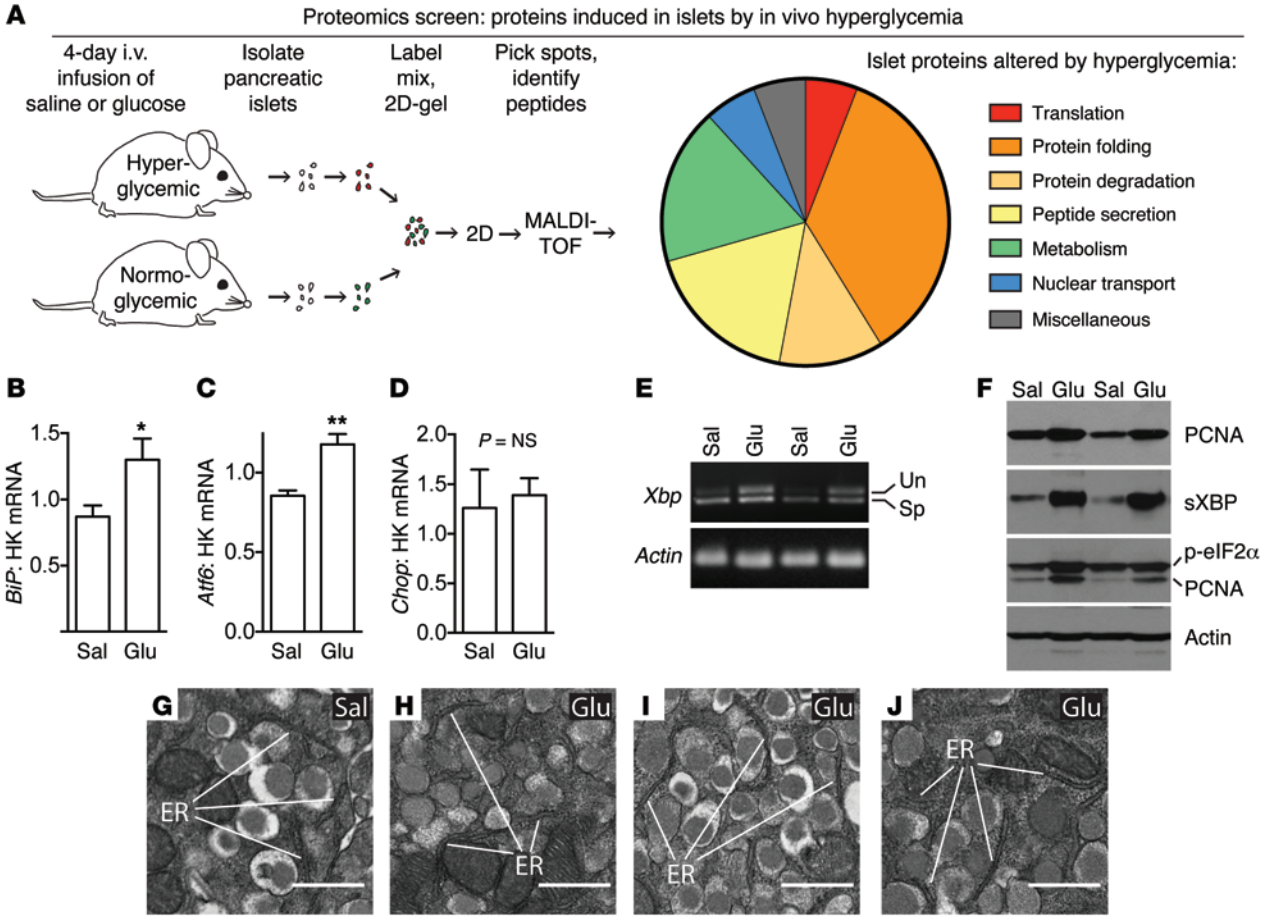

Figure 1. Proteomics screen of islets under proliferative conditions reveals activation of UPR without ER decompensation. (**A**) Proteomics screen on islets after 4 days of in vivo hyperglycemia suggested activation of secretory-pathway peptide synthesis and UPR. (**B**–**E**) RNA analysis of islets after in vivo glucose exposure confirmed activation of UPR (*BiP*, *Atf6*, s*Xbp*) without decompensation (CHOP; $n = 4$–8). (**F**) Immunoblot confirmed increased proliferation (PCNA) and increased sXBP and p-eIF2α at the protein level ($n = 4$). PCNA band is seen in the p-eIF2 blot because PCNA was probed first and the membrane was not stripped. Quantifications of immunoblots are in Supplemental Figure 1. (**G**–**J**) Transmission electron microscopy of pancreas after infusion showed normal, nondilated rough ER in β cells in hyperglycemic mice, confirming the absence of decompensated ER stress (representative images; $n = 3$ glucose infused mice [Glu] and $n = 4$ controls [Sal] were evaluated). HK, housekeeping gene. Data are represented as mean ± SEM; $^*P < 0.05$, $^{**}P < 0.01$ by Student's *t* test. Un, unspliced; Sp, spliced. Scale bars, 500 nm.

available online with this article; doi:10.1172/JCI79264DS1) and a 2D gel-based proteomics screen was performed (Figure 1A and Supplemental Table 1). A majority of proteins with altered expression were related to peptide synthesis and secretion pathways, including ER resident proteins and classic UPR indicator BiP (also called GRP78, which was originally found to be induced during glucose starvation; ref. 26) and PDIA3-ERp57, another sensitive early indicator of ER stress response activation (27). RNA analysis confirmed that UPR was active in islets during in vivo glucose exposure, with increased *BiP*, *Atf6*, and spliced *Xbp* (s*Xbp*) (Figure 1, B–E). Consistent with the low rate of β cell death in this model (15, 24), *Chop*, a marker of decompensated ER stress, was not elevated (Figure 1D). Immunoblot of islets isolated after infusion also showed UPR activation by in vivo hyperglycemia, with increased phosphorylation of transcription of eukaryotic initiation fator 2α (p-eIF2α) and sXBP, as well as proliferation marker PCNA (Figure 1F and Supplemental Figure 1, D–F). Transmission electron microscopy confirmed the absence of morphological evidence of decompensated ER stress in β cells after exposure to mild hyperglycemia in vivo (Figure 1, G–J). Thus, moderate continuous hyperglycemia in vivo, a condition that stimulates β cell proliferation, also leads to UPR activation without decompensation.

To facilitate testing the relationship between UPR and proliferation, an ex vivo model was developed in which freshly isolated primary dispersed mouse islet cells were cultured in low or high glucose. Ex vivo glucose exposure recapitulated the in vivo induction of peptide folding, ER-associated degradation, and secretory pathway members detected in the proteomics screen (Supplemental Figure 2A). Glucose treatment increased proliferation, as measured by BrdU (Figure 2, A and B), *Ki67*, and *Pcna* (Figure 2, C and D). Glucose also induced the UPR, as indicated by increased abundance of *BiP* and calreticulin (Figure 2E), s*Xbp* (Figure 2F), p-eIF2α, ATF6 (Figure 2, G and H), and known transcriptional targets of ATF6 and XBP (Figure 2, I and J), while reducing decompensation marker CHOP (Figure 2K; quantifications of these immunoblots, and additional data, are found in Supplemental Figure 2, B–K, and Supplemental Figure 3). Thus, pancreatic islets responding to increased insulin demand created

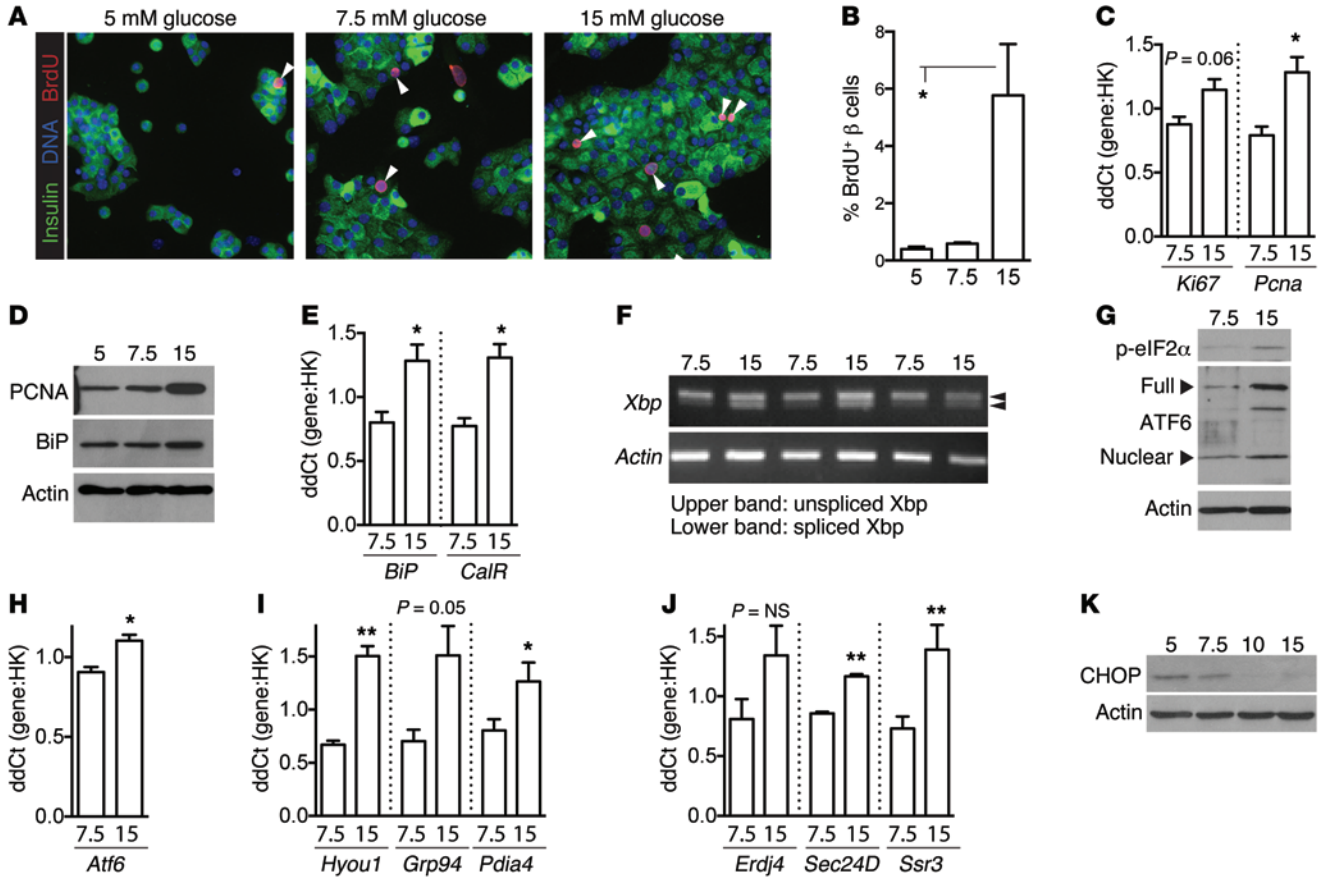

Figure 2. Ex vivo proliferative glucose treatment activates islet cell UPR without decompensation. (**A**–**K**) Mouse islets were dispersed and cultured on uncoated glass (**A** and **B**) or plastic (**C**–**K**) for 72 hours (**A**, **B**, **D**, **G**, and **K**) or 48 hours (**C**, **E**, **F**, and **H**–**J**). β cell proliferation increased in 15 mM glucose as measured by BrdU incorporation (**A** and **B**; $n = 3$) and by abundance of proliferation markers Ki67 and PCNA by qPCR (**C**; $n = 3$) or immunoblot (**D**). Arrowheads in **A** indicate BrdU-positive β cells. UPR markers BiP and calreticulin (CalR) were increased in proliferating islet cell cultures (**D**, immunoblot; **E**, qPCR, $n = 3$). All 3 classical UPR pathways were activated in 15 mM glucose: s*Xbp* (**F**; RNA assay, $n = 3$), p-eIF2α (**G**, immunoblot), and ATF6 (**G**, immunoblot; **H**, qPCR, $n = 3$), as well as ATF6 and XBP transcriptional targets (**I** and **J**, $n = 3$). Decompensation marker CHOP was highest in 5 mM glucose (**K**). Immunoblots in **D**, **G**, and **K** are representative examples of $n = 5$–9 independent replicates; quantifications for **D**, **F**, **G**, and **K** are found in Supplemental Figure 2. HK, housekeeping gene. Images in **A** acquired at ×200 magnification. (**A**–**K**) The numbers 5, 7.5, and 15 refer to glucose concentration. Data are represented as mean ± SEM; $^*P < 0.05$ and $^{**}P < 0.01$ by Student's *t* test.

by hyperglycemia in vivo or in vitro activate both proliferation and UPR without decompensation.

β cells with active UPR are more likely to proliferate. Islets contain a mixed population of cells, including considerable heterogeneity among β cells themselves. Within the β cell population, we hypothesized that some cells might activate UPR due to increased insulin production, while a different subpopulation might respond by proliferating. To assess UPR activation on a per-cell basis, pancreas sections were immunostained for BiP. BiP expression was heterogeneous among insulin-positive cells, and exposure to hyperglycemia in vivo increased the proportion of β cells with high BiP expression (Figure 3, A and B). In vitro glucose treatment also increased the number of β cells containing high levels of BiP (Figure 3C). To determine whether β cells with active UPR were the same or different β cells than those that proliferate, pancreas sections were coimmunostained for insulin, BiP, and PCNA. Surprisingly, visual observation suggested that many β cells positive for PCNA also had high BiP expression (Figure 3, D–G). Quantification confirmed that β cell proliferation was actually more frequent in cells with evidence of active UPR in mice exposed to hyperglycemia (Figure 3H). This relationship was absent in unstressed normoglycemic mice (saline infusion, Figure 3H). To learn whether this observation was unique to the hyperglycemic environment or might be a feature of increased insulin demand, we repeated the experiment in a second model of β cell adaptation, the high-fat diet–fed mouse (HFD-fed mouse) (28). β cell proliferation was more frequent in cells with active UPR in these mice, as well (Figure 3I), despite having normal blood glucose (control diet 144 ± 8 mg/dl, high-fat diet 127 ± 11 mg/dl), suggesting that increased proliferation in β cells with active UPR may be a general feature of insulin-demand compensation.

We confirmed the correlation between active UPR and proliferation in primary dispersed mouse β cells in vitro. Culturing mouse islet cells in 15 mM glucose increased both β cell proliferation and total cell number (Figure 3, J and K). In these cultures also, cells with high BiP levels were more likely to incorporate BrdU (Figure 3, L–N). To test whether UPR activation might be a consequence of preparing to enter the cell cycle, we assessed BiP levels in β cells induced to proliferate by direct manipulation of the cell cycle. In β cells overexpressing cyclin D2, many BrdU-incorporating cells had medium or low levels of BiP, arguing

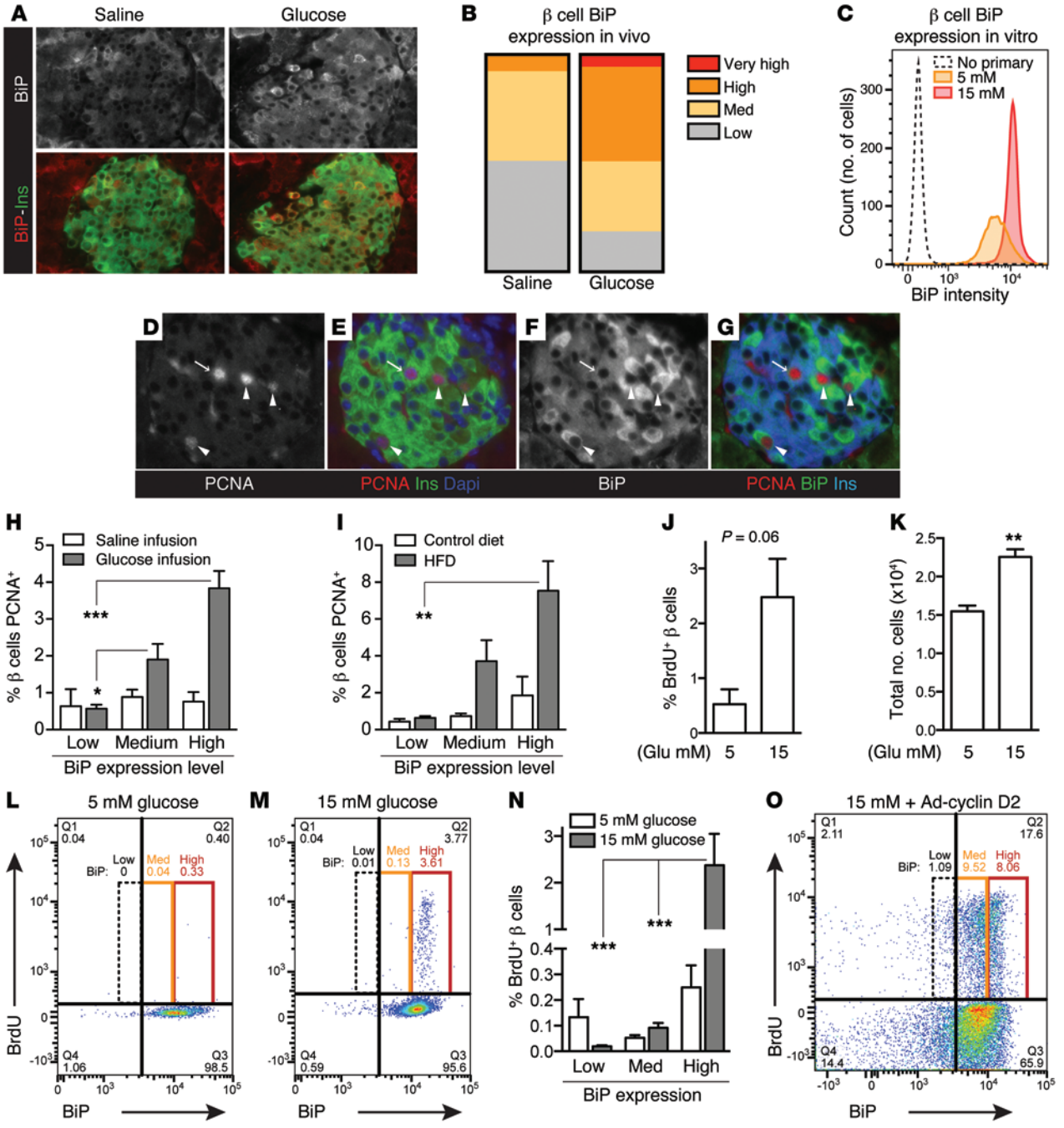

Figure 3. β cells that activate UPR during increased insulin demand are more likely to proliferate. (**A** and **B**) β cell BiP expression was heterogeneous in pancreas sections from glucose-infused mice; hyperglycemia increased the number of β cells with high BiP expression. Representative images are shown from $n = 3$ (saline) and $n = 4$ (glucose) mice. (**C**) In vitro, glucose increased the number of primary mouse islet cells (gated insulin [+]) with high BiP expression. (**D**–**G**) In pancreas sections from hyperglycemic mice, PCNA staining frequently occurred in β cells with high BiP expression (arrowheads) and less frequently in β cells with low BiP expression (arrows). (**H** and **I**) In pancreas sections from hyperglycemic (**H**) or high-fat fed (**I**) mice, β cells containing high BiP were more likely to be PCNA-positive ($n = 3$–5). (**J** and **K**) In vitro, by flow cytometry, glucose increased primary mouse β cell BrdU incorporation and cell number ($n = 3$). (**L**–**N**) Under glucose stimulation, mouse β cells with high BiP were more likely to be BrdU-positive ($n = 3$). (**O**) In contrast, in primary mouse β cells overexpressing cyclin D2, BrdU incorporation was not limited to high BiP–expressing cells. (**A** and **D**–**G**) Images acquired at ×200 magnification. Images in **D**–**G** and flow plots in **C**, **L**, **M**, and **O** are representative of $n = 3$–5 experiments. Data are represented as mean ± SEM; $^*P < 0.05$, $^{**}P < 0.01$, and $^{***}P < 0.001$ by ANOVA (**H**, **I**, and **N**) or Student's *t* test (**J** and **K**).

against the explanation that a correlation between BiP and proliferation is due to induction of BiP during proliferation (Figure 3O). Taken together, we conclude that β cells with active UPR are more likely to proliferate than β cells without active UPR.

Gentle UPR activation increases β cell proliferation in vitro in the context of high glucose. Despite the abundant evidence in the literature that decompensated ER stress causes β cell death (3–7), the observed correlation between UPR and proliferation led us to

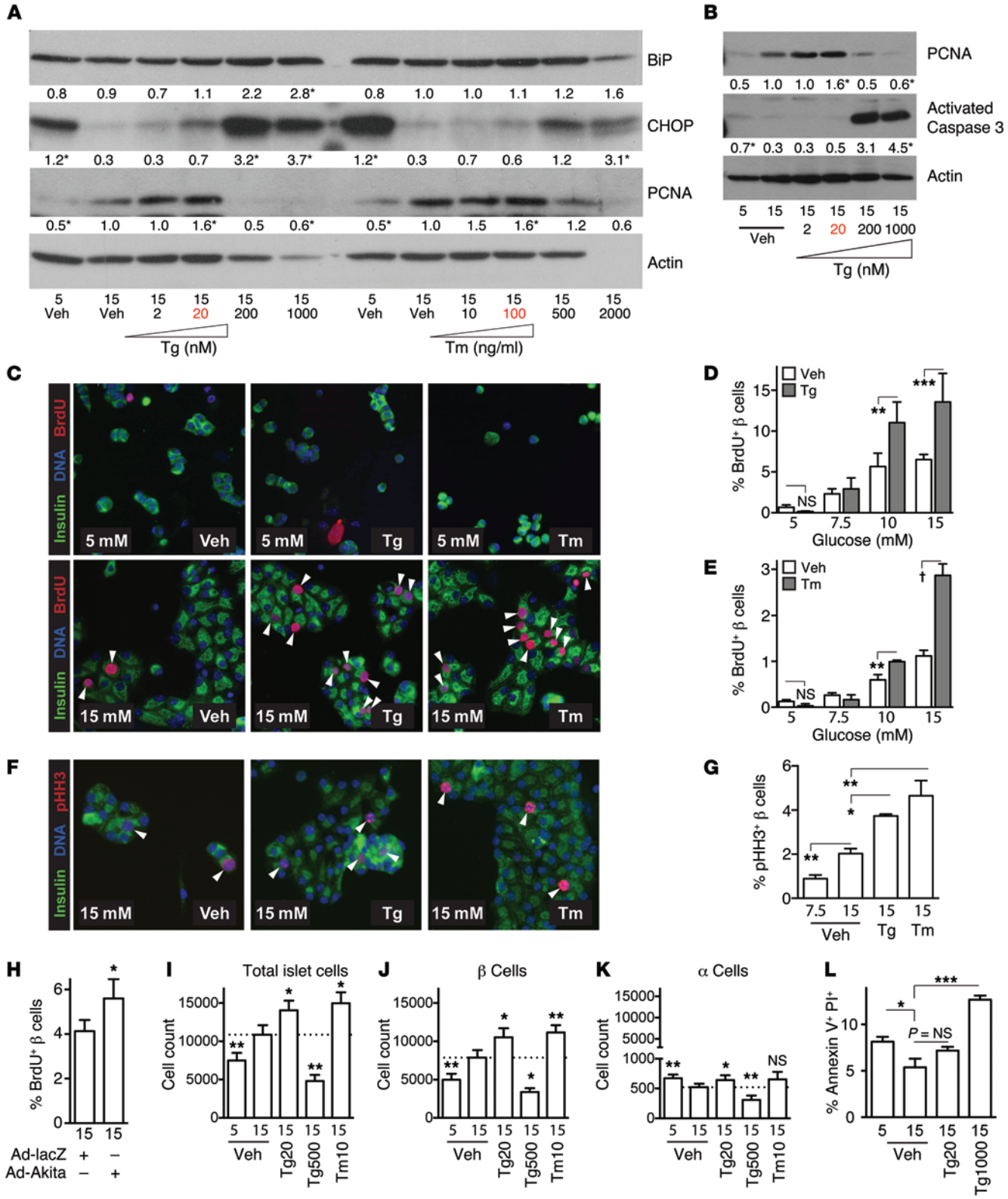

Figure 4. Activating mild UPR ex vivo increases β cell proliferation and β cell number. (**A** and **B**) In primary mouse islet cells, PCNA induced by 15 mM glucose was further increased by low-dose Tg (2–20 nM) or Tm (10–100 ng/ml). A marked drug-dose threshold was apparent; at higher doses of Tg or Tm, PCNA was abruptly lost and decompensation markers CHOP (**A**) and activated caspase 3 (**B**) were induced. Numbers below bands are average band intensity quantification of n = 5–7 immunoblots; plots of averages are found in Supplemental Figure 4. *P < 0.05 vs. 15 mM vehicle. (**C**–**E**) Mouse islet cells treated with low-dose Tg or Tm increased proliferation in high glucose (n = 3). (**F** and **G**) Proliferation was confirmed by phospho-Histone H3 (n = 3). (**H**) Expression of Akita proinsulin increased β cell proliferation (n = 5). (**I**–**L**) Quantitative cell counting using flow cytometry showed increased β cell number in cultures treated with low-dose Tg and Tm (n = 5–7). (**J** and **K**) Low-dose Tg did not induce cell death (n = 4). (**C** and **F**) Images acquired at ×200 magnification. Data are represented as mean ± SEM; *P < 0.05, **P < 0.01, ***P < 0.001, and †P < 0.0001 by ANOVA. P values in **A**, **B**, **G**, and **I**–**L** are vs. 15 mM vehicle.

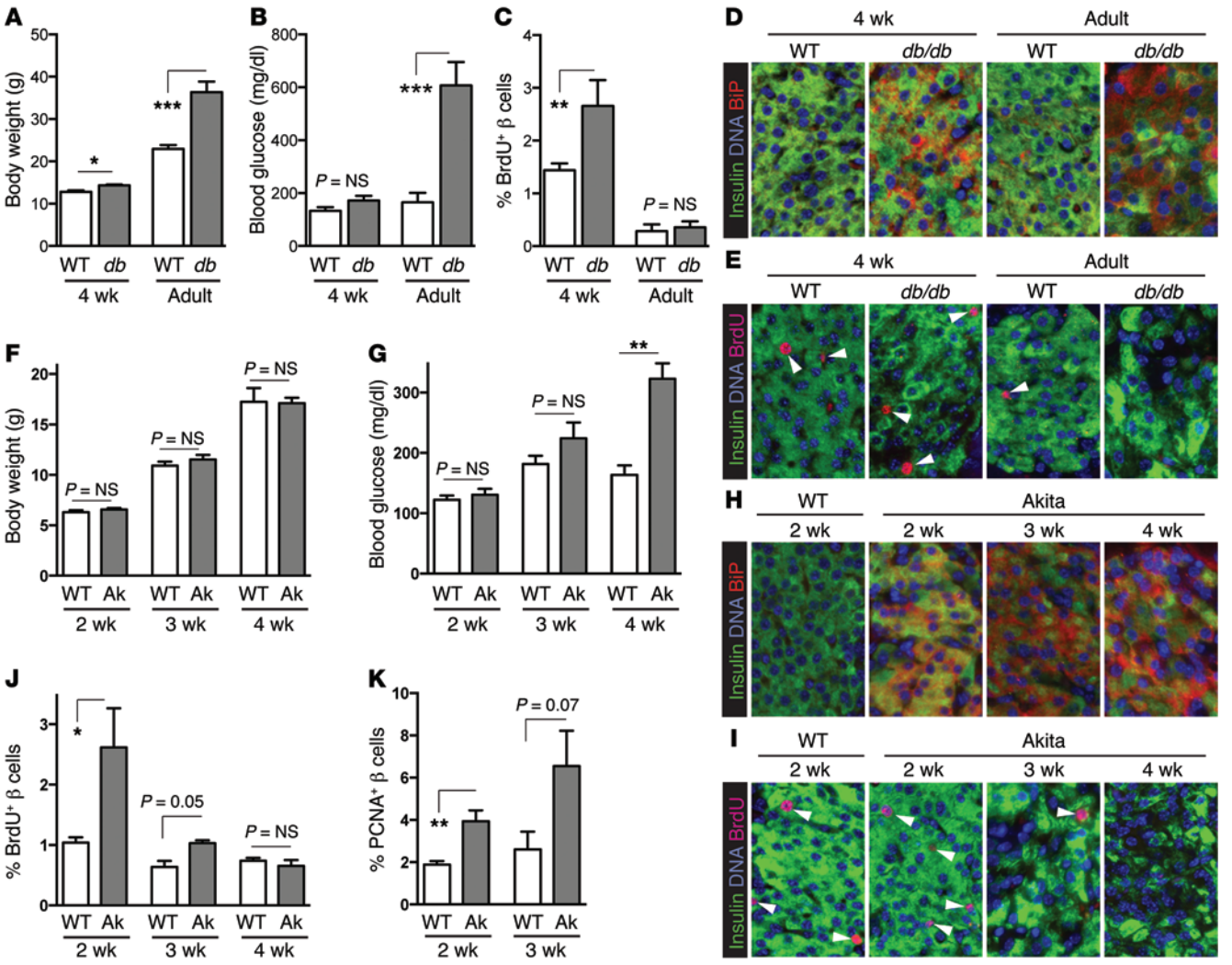

Figure 5. In vivo ER stress increases β cell proliferation before decompensation. (**A**–**E**) *db/db*/BLKS mice have increased β cell proliferation when UPR is present but before islet decompensation occurs. (**A** and **B**) Body weight and blood glucose were near normal in *db/db* mice at 4 weeks of age, but obesity and diabetes were present at 11–14 weeks of age (adult; n = 3–5). (**C**–**E**) At 4 weeks of age, UPR was already active (**D**), and β cell proliferation was increased (n = 4–6; **C** and **E**). In adult *db/db* mice, proliferation was no longer increased when β cell decompensation was evident (hyperglycemia, loss of islet morphology; n = 6–10). (**F**–**K**) ER stress applied directly to the β cell is sufficient to increase β cell proliferation in vivo. (**F**–**H**) Heterozygous Akita mice had normal blood glucose and body weight at 2 and 3 weeks of age but developed hyperglycemia at 4 weeks (n = 4–22). Pancreas sections showed UPR activation was already present at 2 weeks of age. (**I**–**K**) BrdU incorporation was elevated at 2 and 3 weeks of age, when UPR was active but before decompensation began (n = 3–5). (**K**) Proliferation in Akita β cells at 2–3 weeks of age was confirmed using PCNA staining (n = 5–11). (**D**, **E**, **H**, and **I**) Images acquired at ×200 magnification. Data are represented as mean ± SEM; $^*P < 0.05$, $^{**}P < 0.01$, and $^{***}P < 0.001$ by Student's t test.

consider the hypothesis that modest UPR activation might actually promote β cell proliferation. To test this, primary mouse islet cells were cultured with small molecules that induce ER stress by different mechanisms, by interfering with ER calcium handling (thapsigargin, Tg) or glycosylation (tunicamycin, Tm). Since the usual concentrations of these agents (1 μM for Tg and 1–10 μg/ml for Tm) induce decompensated ER stress and cell death, we applied a broad range of concentrations, starting with 2–3 orders of magnitude lower than the usual dose. Assessing decompensated ER stress by immunoblot for CHOP or caspase 3, we confirmed that these drugs in usual concentrations induce severe ER stress and cell death in primary mouse islet cells (Figure 4, A and B, and Supplemental Figure 4). By PCNA immunoblot, high glucose induced proliferation, as expected. Intriguingly, low doses of either Tg or Tm further increased PCNA abundance in islet cells cultured in 15 mM glucose, with an abrupt dose threshold above which PCNA disappeared and CHOP and caspase 3 were induced. To determine whether increased PCNA abundance in the mixed islet cell population represented increased β cell proliferation, cultures were treated with low-dose Tg or Tm and assayed for proliferation by BrdU incorporation. Remarkably, in 15 mM glucose, both drugs increased mouse β cell proliferation over vehicle control (Figure 4, C–E, and Supplemental Figures 5 and 6). Although the dispersed-islet BrdU proliferation assay produces variable maximum proliferation from one islet prep to the next, despite the multiple precautions taken to standardize this assay (see Methods), a pro-proliferative effect of Tg and Tm was a consistent finding. The proliferative effect was dependent on glucose concentration: in

5 mM glucose (usual islet culture medium), low-dose Tg and Tm induced visible toxicity with cell loss and absence of proliferation, while a proliferative effect was seen in 10–15 mM glucose. Given concerns in the field that BrdU incorporation does not always indicate cell proliferation, we further confirmed the PCNA immunoblot and BrdU immunostaining with phospho-histone H3 (pHH3) immunostaining, a marker of mitosis. Both Tg and Tm increased the percent of β cells staining for pHH3 (Figure 4, F and G). To test whether directly stressing the ER could increase β cell proliferation, mouse islet cells were transduced with adenovirus expressing *Ins2*^{C96Y} (Akita). Akita proinsulin expression also increased β cell BrdU incorporation (Figure 4H). In addition to histochemical assessment of proliferation, we hypothesized that increased proliferation should increase the number of cells in the culture wells. By flow cytometry, culture in 15 mM glucose increased the number of islet cells and β cells, but not α cells, over 5 mM controls (Figure 4, I–K, and Supplemental Figures 6 and 7). Low-dose Tg and low-dose Tm, but not high-dose Tg, increased the number of β cells in the culture wells, again supporting a proliferative effect. Comparative cell counts include both addition of proliferating cells in some samples and loss of dying cells in others, such as in the 5 mM glucose condition (see below). Although we did not expect low-dose Tg and Tm exposure to cause cell death, because CHOP and activated caspase 3 were low (Figure 4, A and B), we directly measured cell death by Annexin V/propidium iodide staining (Figure 4L and Supplemental Figure 8). As expected, cell death was strongly detected in the positive control (high-dose Tg) but was low in primary islet cells exposed to proliferative-dose Tg, comparable to 15 mM glucose control. Cell death was increased in the 5 mM glucose condition, possibly explaining the apparent heightened sensitivity to Tg and Tm in low glucose, and contributing to the difference in cell number between 5 mM and 15 mM glucose on flow counts. Finally, to exclude the possibility that BrdU incorporation was an artifact of DNA damage, cultures were coimmunostained for BrdU and γ-H2AX. After treatment with glucose or proliferative doses of Tg or Tm, the majority of BrdU-positive nuclei were negative for γ-H2AX (Supplemental Figure 9). Taken together, these data suggest that inducing mild, nondecompensated ER stress, by interfering with 2 distinct ER maintenance systems, is sufficient to induce β cell proliferation in glucose-dependent fashion in vitro.

In vivo ER stress induces β cell proliferation before decompensation. Since in vitro experiments suggested that adaptive UPR activation increased proliferation, we asked whether stressing the ER might drive β cell proliferation in vivo. We first studied leptin-receptor–deficient *db/db* mice on the C57BLKS genetic background. These mice are a well-established β cell ER stress model, due to a combination of elevated insulin demand from insulin resistance and the C57BLKS genetic influence, which is predisposed to β cell ER stress and failure (29–32). At 4 weeks of age, *db/db* mice still had near-normal body weight and blood glucose, but they showed UPR activation as determined by BiP immunostaining (Figure 5, A–D). Consistent with the hypothesis that early or mild UPR promotes proliferation, β cell proliferation was increased in *db/db* mice at 4 weeks of age but declined to the same level as controls in adulthood when mice became obese and diabetic, and when islets showed β cell loss (Figure 5, A–E). Thus, in the *db/db*-C57BLKS model of β cell stress, β cell proliferation increased early (when UPR was present but of lower intensity or shorter duration), but proliferation was lost later when decompensation occurred (when stress was of greater intensity or prolonged).

To determine whether ER stress applied directly to the β cell increases β cell proliferation in vivo, we studied heterozygous *Ins2*$^{C96Y/+}$ (herein referred to as Akita) mice, in which a mutant proinsulin (1 of 4 insulin alleles) causes β cell ER stress due to improper disulfide formation (32, 33). These mice are born with normal glucose tolerance but become diabetic by adulthood due to ER stress–induced β cell failure (34, 35). In our colony, body weight and blood glucose in Akita pups were normal at 2 and 3 weeks of age, with onset of diabetes at 4 weeks (Figure 5, F and G). Immunostaining for BiP showed that UPR was active as early as 2 weeks of age, with abnormal β cell morphology (uneven insulin staining) developing at 3–4 weeks (Figure 5, H and I). Again consistent with our hypothesis, β cell proliferation, as measured by BrdU incorporation and confirmed by PCNA staining, was increased at 2 weeks, less so at 3 weeks, and was no longer elevated at 4 weeks, when severe stress was evident (Figure 5, I–K). Thus, β cell proliferation was elevated in both *db/db* and Akita mice early after the onset of ER stress but was lost when islets decompensated. In sum, 4 distinct ER stressors — interference with ER calcium handling, blockage of ER protein glycosylation, leptin-receptor deficiency in a β cell ER stress–sensitive background, and loading of misfolded proinsulin in the ER — all resulted in increased β cell proliferation. These data are consistent with the hypothesis that mild or early UPR promotes β cell proliferation.

UPR activation is required for insulin-demand–induced β cell proliferation in vitro and in vivo. To learn whether UPR activation is required for the β cell proliferative response to glucose ex vivo, we applied 2 chemical chaperones — tauroursodeoxycholic acid (TUDCA) and 4-phenylbutyrate (PBA), which reduce ER stress — to islet cell cultures. Both chemical chaperones reduced glucose-induced ER stress in islet cultures, with reductions in p-eIF2α, p-IRE1, and ATF6 (Figure 6A). Immunoblot for PCNA suggested that both chaperones also reduced glucose-induced islet cell proliferation (Figure 6, B and C). Using immunofluorescence to evaluate chaperone effects specifically on β cell proliferation, we confirmed that addition of either chaperone prevented the increase in β cell proliferation induced by glucose (Figure 6, D and E). To exclude the possibility that the drugs nonspecifically inhibit some mechanism required for cell division or incorporation of the BrdU label, we repeated the experiment while activating the cell cycle by overexpressing cyclin D2. The chaperones again blocked proliferation induced by glucose but had no effect on BrdU incorporation in islet cells overexpressing cyclin D2, suggesting the result was not due to nonspecific toxicity (Figure 6, F and G).

To test whether ER stress is required for insulin-demand–induced β cell proliferation in vivo, mouse models with increased β cell ER load were treated with control or i.p. TUDCA injections for 2 days prior to euthanasia. Immunofluorescence of pancreas sections showed that TUDCA exposure reduced the abundance of ER stress marker BiP in β cells (Figure 7A). TUDCA treatment significantly reduced β cell proliferation in Akita (Figure 7, B and C), *db/db*-BLKS (Figure 7, D and E), and HFD-fed mice (Figure 7, F and G), without lowering blood glucose over this time frame (Supplemental Figure 10) or preventing intestinal BrdU incor-

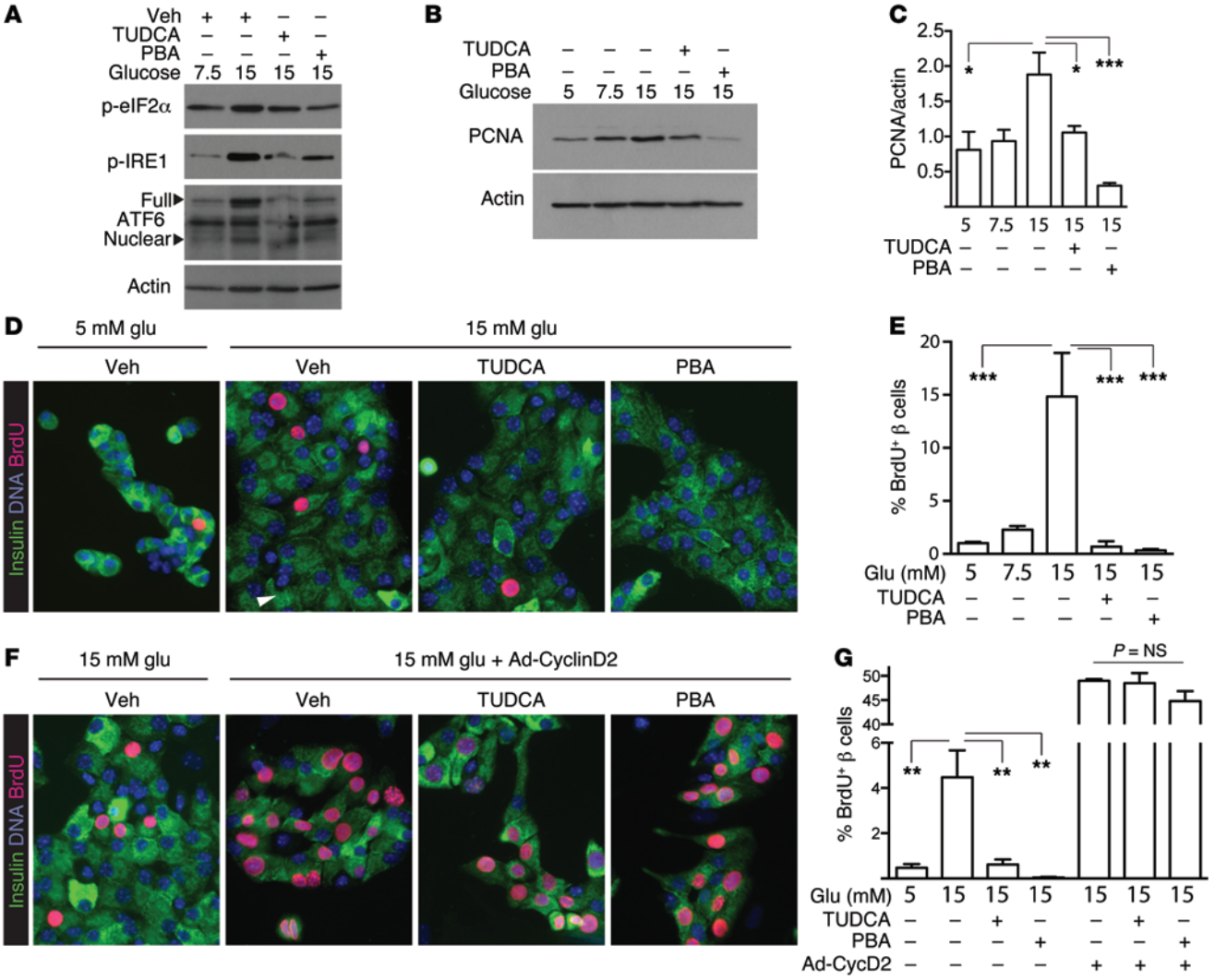

Figure 6. UPR activation is required for glucose-induced β cell proliferation ex vivo. (**A**) Chemical chaperones TUDCA and PBA reduced mouse islet cell UPR activation by 15 mM glucose. (**B** and **C**) Glucose induction of PCNA was reduced by chaperones TUDCA and PBA. Immunoblots in **A** and **B** are representative of n = 3–4 independent experiments. (**D** and **E**) Relieving ER stress with either TUDCA or PBA prevented glucose-induced proliferation in mouse β cells (n = 4). (**F** and **G**) Neither TUDCA nor PBA reduced proliferation induced by overexpressing cyclin D2, arguing against a nonspecific toxic effect on BrdU uptake or proliferation (n = 3). Data are represented as mean ± SEM; $^{*}P < 0.05$, $^{**}P < 0.01$, and $^{***}P < 0.001$ by ANOVA.

poration (Rohit Sharma, unpublished observations). Taken with the caveats that small-molecule inhibitors may have off-target effects on other pathways or tissues and that TUDCA may reduce metabolic demand in high-demand states, such as HFD-fed or *db/db* mice (36), these results suggest that UPR activation may be required for insulin demand or ER stress–driven β cell proliferation in vivo.

ATF6 is necessary and sufficient to drive β cell proliferation. Three canonical pathways constitute the UPR response: PERK/eIF2α, IRE1/XBP1, and ATF6 (3, 7). All 3 of these pathways were activated by glucose in primary mouse islet cell cultures (Figure 2, F–J). To determine whether one or more of these pathways mediate the proliferative response to glucose in the β cell, each pathway was inhibited individually in primary mouse islet cells using small molecules (Supplemental Figures 3 and 11; refs. 37–39). Glucose-induced proliferation was reduced by both the ATF6 and IRE1 inhibitors, but was not affected by the PERK inhibitor (Figure 8A). In contrast, none of these inhibitors reduced cell-cycle entry caused by cyclin D2 overexpression, arguing against nonspecific toxicity (Figure 8A). Immunoblots showed that the ATF6 and IRE1 inhibitors, but not the PERK inhibitor, also reduced PCNA abundance in primary islet cell cultures (Figure 8B). To test whether activating the IRE1 or ATF6 pathways induced β cell proliferation, electroporation was used to overexpress IRE1, spliced (active) XBP1, or ATF6 in primary mouse islet cells (Figure 8, C–G, and Supplemental Figure 12). Surprisingly, given that the IRE1 inhibitor reduced proliferation, overexpression of either IRE1 or sXBP1 also reduced β cell proliferation in 15 mM glucose (Figure 8, D and G). ATF6 overexpression, however, was sufficient to increase β cell proliferation (Figure 8G). To test whether IRE1 or ATF6 were required for glucose-induced proliferation, expression was reduced in dispersed islet cells using shRNA (Figure 8, H–P). Similar to the inhibitor experiment, knockdown of either ATF6 or IRE1 expression reduced glucose-induced BrdU incorporation

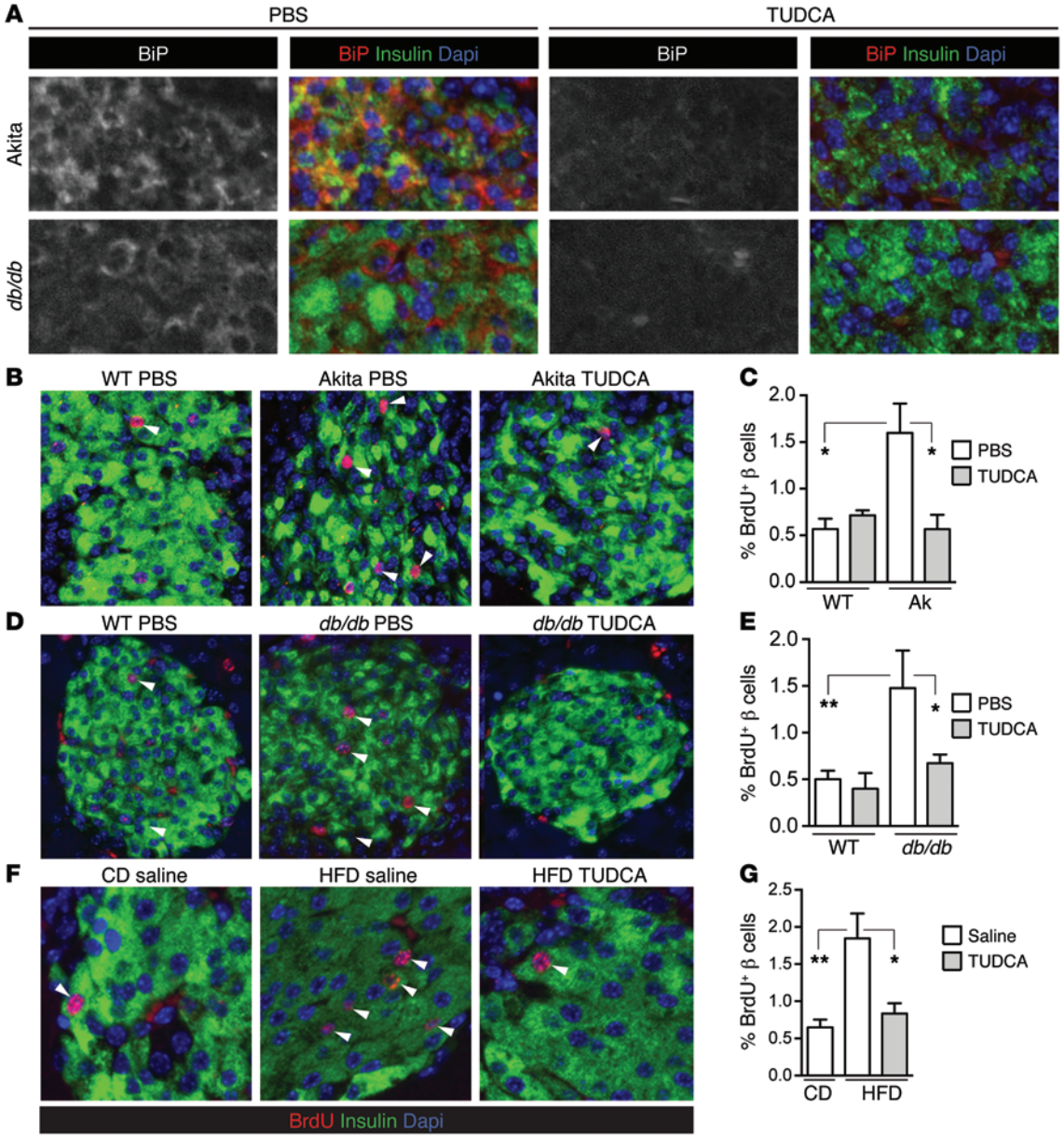

Figure 7. UPR activation is required for insulin demand–induced β cell proliferation in vivo. (**A**) Twice daily i.p. injections of TUDCA for 2 days prior to euthanasia reduced β cell ER stress marker BiP in Akita and *db/db*-BLKS ER load models. Images are representative of $n = 3$ biological replicates. (**B**–**G**) Two days of twice daily i.p. TUDCA reduced β cell proliferation in 2-week-old Akita mice (**B** and **C**; $n = 3$–5), in 4-week-old *db/db* mice (**D** and **E**; $n = 5$–13), and in HFD-fed mice (**F** and **G**; $n = 5$–8). Images were acquired at ×200 magnification. Arrowheads point to BrdU-positive β cells. Data are represented as mean ± SEM; $^{*}P < 0.05$ and $^{**}P < 0.01$ by ANOVA.

(Figure 8, I and J). However, only ATF6 knockdown significantly decreased PCNA abundance (Figure 8, K–P). In sum, these results suggest that ATF6 is necessary and sufficient for glucose-induced proliferation in mouse β cells and that IRE1/XBP perturbation in either direction interferes with proliferation, but the pathway is not sufficient to drive proliferation.

UPR modulates proliferation in human β cells. Given the important differences between mouse and human β cells (40, 41), findings in mice must be tested in human samples to confirm potential medical relevance. We tested islet cells from 12 human donors (Supplemental Tables 2 and 3) to see whether UPR regulates β cell proliferation. Dispersed islet cells were cultured on glass coverslips in the presence of 7.5 or 15 mM glucose, plus activators or inhibitors of UPR (Figure 9, A–G). Proliferation increased in β cells from all donors when exposed to 15 mM glucose, although the basal proliferation and degree of increase varied considerably among donors (Supplemental Figure 13). To determine whether UPR activation could increase proliferation in these samples, Tg and Tm were applied. Tg and Tm increased BiP abundance in human islet cells (Supplemental Figure 14). β cells from most donors increased proliferation when treated with low-dose UPR-inducing agents (Figure 9, C and D). Due to the prominent variability in human islet preparations, the results are expressed as normalized to the rate of proliferation

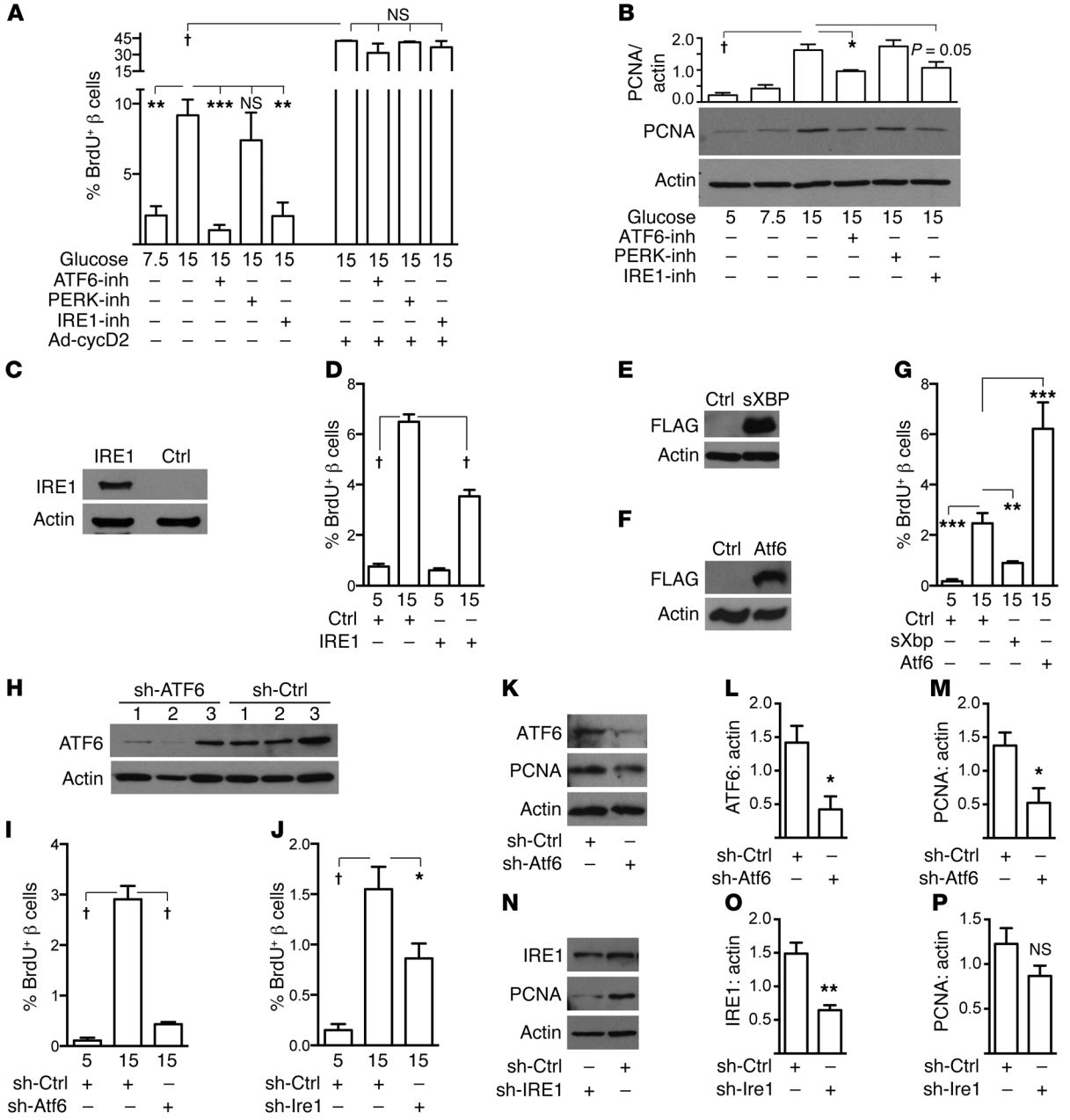

Figure 8. The ATF6 pathway is necessary and sufficient for glucose-induced β cell proliferation in vitro. (**A**) In primary mouse β cells, proliferation induced by glucose was markedly reduced by small-molecule inhibitors of the ATF6 and IRE1 pathways, but not by a PERK inhibitor (n = 3–4). Direct cell-cycle activation by overexpression of cyclin D2 was unaffected, arguing against nonspecific toxicity. (**B**) Immunoblot showed that glucose-induced islet cell PCNA was reduced by both the ATF6 and IRE1 inhibitors (n = 3). (**C**–**G**) Overexpression of IRE1, (n = 3, **C** and **D**), sXBP1 (n = 4, **E** and **G**), or ATF6 (n = 4, **F** and **G**) in mouse islet cells showed that only ATF6 increased β cell proliferation. (**H**–**P**) shRNA knockdown of ATF6 or IRE1 in primary mouse islet cells revealed that optimal levels of both ATF6 and IRE1 are required for glucose-induced β cell proliferation (n = 3–6, **I** and **J**), although only ATF6 knockdown reduced PCNA abundance (n = 3–5, **K**–**P**). **H** shows knockdown for **I**; **K** for **L** and **M**; and **N** for **J**, **O**, and **P**. The duration of all experiments was 72 hours. Data are represented as mean ± SEM; $^{*}P < 0.05$, $^{**}P < 0.01$, $^{***}P < 0.001$, and $^{\dagger}P < 0.0001$ by ANOVA (**A**, **B**, **D**, **G**, **I**, and **J**) or Student's t test (**L**, **M**, **O**, and **P**).

in 7.5 mM glucose (raw data in Supplemental Figure 13). Islets from a single T2D donor were included; these β cells showed no proliferative response to UPR activation. γ-H2AX was detected infrequently in human islet cultures and did not colocalize with BrdU immunofluorescence in low-dose Tg- and Tm-treated cultures, suggesting the observed BrdU incorporation was not due to DNA damage (Supplemental Figure 15). β cells from 5 of 6 donors tested showed a reduction in glucose-induced proliferation when treated with TUDCA or PBA (Figure 9E and Supplemental Figures 13 and 14), suggesting the UPR may be required for glucose-induced proliferation in human β cells. To determine whether ATF6 mediates the proliferative response to glucose, human islet cell cultures were treated with either ATF6 inhibitor or overexpression of human *ATF6* by adenovirus. Inhibiting ATF6 reduced proliferation in 15 mM glucose (Figure 9F) and overexpression of *ATF6* increased proliferation in 15 mM glu-

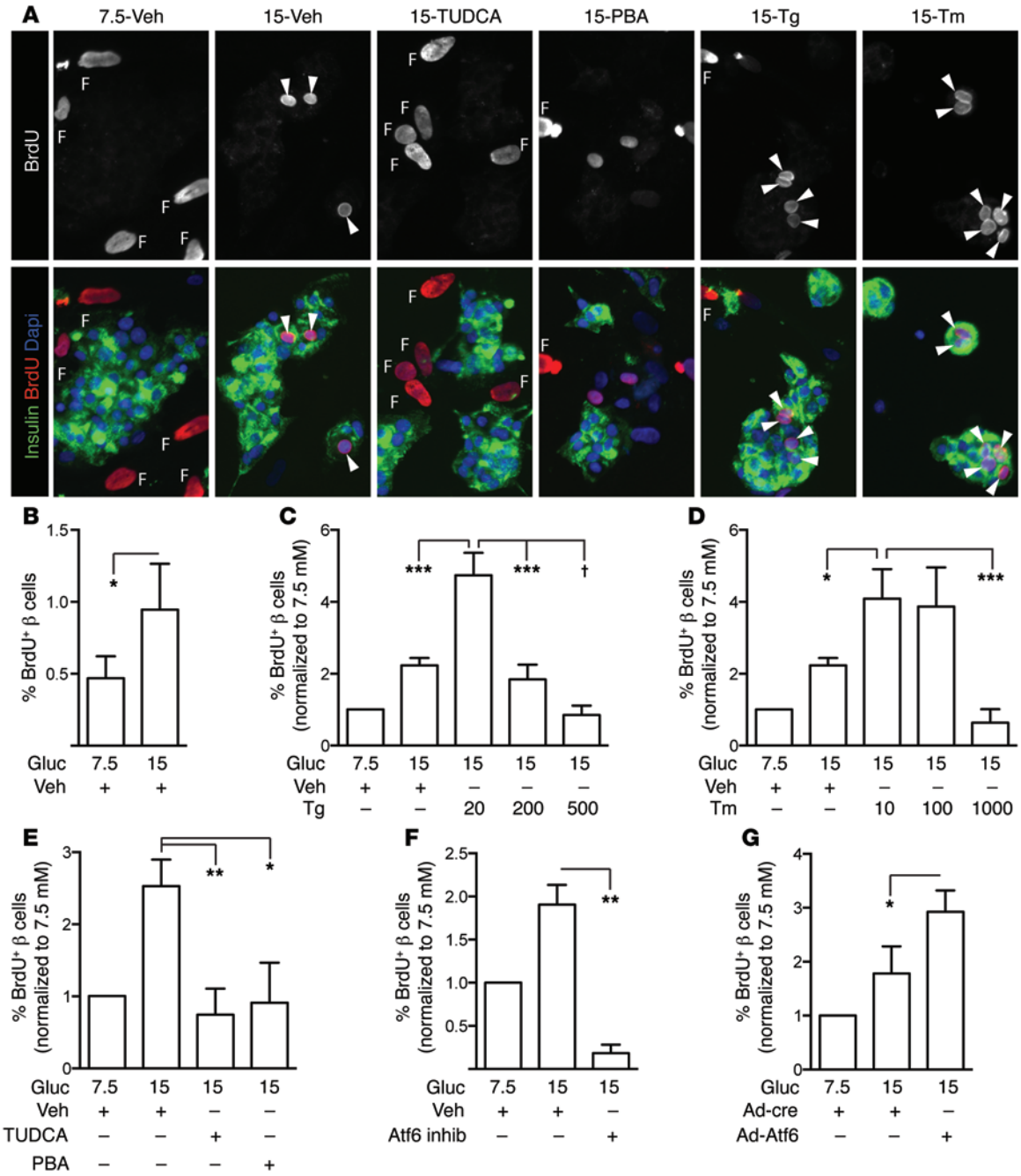

Figure 9. UPR is necessary and sufficient to increase human β cell proliferation, via ATF6. (**A**) Human islets were dispersed and cultured on glass coverslips for 96 hours, with BrdU added to culture medium for the entire duration. Arrowheads indicate BrdU-positive β cells. Fibroblast nuclei, which are larger than endocrine nuclei, are labeled F. (**B**) Human β cell proliferation increased in high glucose (n = 12). Because baseline proliferation varied widely among donors, subsequent panels show data normalized to the 7.5 mM proliferation rate. The raw, nonnormalized data for each prep are in Supplemental Figure 13. (**C** and **D**) Low-dose Tg (20 mM, **C**) or Tm (10–100 ng/ml, **D**) increased human β cell proliferation (n = 6–12). (**E**) TUDCA and PBA reduced human β cell proliferation in 15 mM glucose (n = 6). (**F** and **G**) In 15 mM glucose, human β cell proliferation decreased in the presence of the ATF6 inhibitor (n = 7; **F**) and increased with overexpression of ATF6 (n = 4; **G**). (**A**) Images acquired at ×200 magnification. Data are represented as mean ± SEM; $^{*}P < 0.05$, $^{**}P < 0.01$, $^{***}P < 0.001$, and $^{\dagger}P < 0.0001$ by ANOVA (**C**–**E**) or Student's t test (**B**, **F**, and **G**).

cose (Figure 9G), suggesting that ATF6 promotes human β cell proliferation. In sum, these results suggest that human β cell proliferation may be regulatable by modulating UPR in general and ATF6 activity in particular. Figure 10 illustrates the concept of a therapeutic window of β cell stress that could be harnessed to expand β cell mass to prevent or treat diabetes.

Discussion

Our observations link UPR activation in the β cell with the well-documented demand-driven proliferative expansion of β cell mass. The work presented here has several strengths. The hypothesis arose from an unbiased protein-based screen. The connection between UPR and demand-led β cell proliferation was tested both

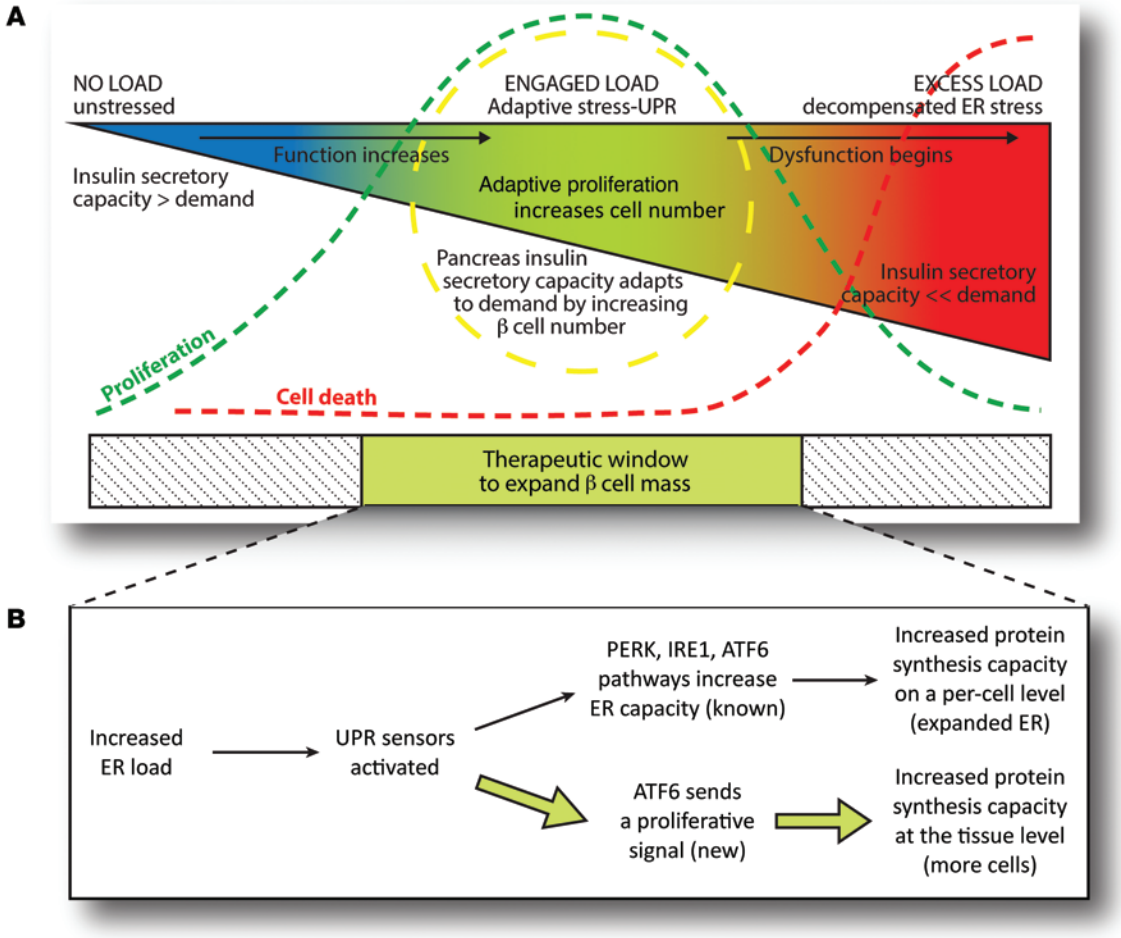

Figure 10. Model: How one secretory cell type, the β cell, links protein synthesis demand to increased cell number through proliferation. (**A**) The β cell stress continuum. It was previously known that excess ER load results in β cell dysfunction and death. The current study adds a new concept, in which moderate ER load, known to promote functional adaptation of ER capacity, also leads to tissue adaptation of β cell number through proliferation. This continuum illustrates a potential therapeutic window of stress that might be targeted to promote β cell mass expansion. (**B**) Schematic illustrating how UPR activates proliferation in β cells.

in vitro and in vivo, using multiple tools that impact ER biology by different mechanisms. Using small molecules and genetic experiments in vitro, the proliferative signal was traced to the ATF6 branch of the UPR. Findings were extended to human islets.

Taken together, these studies have important implications. First, we have identified a new role for the classic UPR mechanism: promoting proliferation in tissue homeostasis of a secretory cell type. Although cancer biologists have implicated UPR pathways in tumor cell adaptation and spread (42), this is the first report to our knowledge showing a role for UPR in determining tissue cell number in normal physiology. Cell biologists have established the UPR as a strategy by which cells adapt resources to meet peptide synthesis needs while minimizing unnecessary ER volume (3, 7). To perform this function, UPR senses secretory peptide synthesis overload and triggers new lipid and peptide production to expand ER capacity on a per-cell basis. Our data suggest that UPR load sensors may direct adaptation of peptide synthesis not only at the level of the individual cell, but also at a whole-organ level, by increasing the number of cells through proliferation. Thus, from a physiology perspective, UPR may contribute to determination of organ size.

Linking UPR sensors with β cell mass expansion in response to insulin demand is, in hindsight, an obvious solution to the puzzle of β cell mass regulation. The cell type most tuned to insulin demand is the β cell, through precise glucose sensing. Unmet insulin demand increases proinsulin production at the RNA and protein level, and proinsulin synthesis activates UPR pathways (3, 7, 43). Since β cell mass expansion occurs by proliferation of mature β cells, the simplest model explaining how β cell proliferation initiates in response to insulin demand would invoke a β cell–intrinsic sensor of insulin demand, such as the UPR. Connecting UPR with proliferation may explain why stem cells don't participate in β cell homeostasis because undifferentiated cells would not sense insulin demand. In fact, this concept suggests a new demand-driven model of tissue homeostasis, in which differentiated cells sense an unmet need for their function and produce new cells to meet that need.

Observations from medicine hint that demand-driven determination of organ size might also apply to other tissues and might contribute to some disease processes. Several endocrine cell types proliferate when hormone synthesis increases, including islet α cells as well as thyroid, parathyroid, and pituitary cells (44–47). In

some clinical situations — such as goiter, Nelson's syndrome, and parathyroid hyperplasia — the proliferation may require surgical or other intervention, at some risk to the patient (45, 48). Other non-endocrine cells that produce secretory-pathway peptides may also employ this mechanism. Understanding the root cause of these proliferative conditions is the first step to finding treatments.

Previous observations have hinted that UPR activation in vivo might promote β cell proliferation, although no studies have directly addressed this hypothesis until now. Inducing UPR by transgenic overexpression of mutant proinsulin or the islet amyloid polypeptide (49, 50), or by deletion of ER stress cell-death mediators CHOP or DP5 (30, 51), was noted to increase islet size or β cell proliferation. In adult mice, reducing PERK expression increased β cell proliferation (52, 53). This is consistent with our observation that the PERK pathway is not responsible for the pro-proliferative UPR signal and supports the possibility that ATF6, responding to loss of PERK, might drive proliferation. Deletion of *Xbp1* in β cells resulted in insulin-deficient diabetes, impaired insulin processing, and dilated ER, suggesting decompensated ER stress; β cell proliferation was reduced (54). IRE1 was found to promote prostate cancer cell-line proliferation via XBP1 (55). In our experiments, although IRE1 inhibition reduced β cell proliferation, both IRE1 and XBP1 overexpression also reduced proliferation, a conundrum that is consistent with the known careful balance of IRE1 and XBP actions (54) and that requires further study. Whole-body *Atf6*-null mice have reduced pancreatic insulin content and accelerated decompensation in the setting of insulin resistance, which could be consistent with loss of β cell mass (56); however, mice lacking *Atf6* in β cells are reported to develop normally (57).

In vitro studies in β cells have not thus far reported a pro-proliferative effect of UPR activation. This may be because many investigators use transformed cell lines for in vitro studies, and transformation overrides usual homeostatic proliferation mechanisms. The doses of Tg and Tm usually used in culture cause decompensation and cell death, and the proliferative effect is dependent on glucose concentrations not typically used in routine culture. Culture of primary islet tissue, while more cumbersome and expensive, is more relevant to the in vivo environment, at least with respect to proliferation studies.

In an important clue to the mechanism of this effect, proliferation induced by low-dose ER stressors in vitro was strictly dependent on glucose concentration of the culture medium, with proliferation observed in higher glucose but with decompensation markers and cell death found in lower glucose. Possible explanations for this observation include glucose dependence of stress response parameters and energy requirements of cell division. The glucose concentrations indicated refer to conditions at the start of the experiment; glucose abundance at the end of the experiments was not measured and may have been lower due to utilization. In low glucose, some hallmarks of the integrated stress response (ISR) were induced, including CHOP and cell death, while ATF6 was not increased (Figure 4, A, B, L, and Supplemental Figure 4C). Our findings are consistent with prior observations that ISR is activated in rat islets or the murine min6 pancreatic β cell line at 2 mM and 5 mM glucose, whereas UPR is activated in high glucose (58, 59). Glucose concentration may impact the degree, duration, or identity of transcripts affected by ISR-mediated translation block in β cells (60). Intriguingly, in HEK293T cells, the ISR preferentially reduces translation of MTOR-regulated genes (61); β cell proliferation is strictly dependent on MTOR activation (62). It is possible that glucose uptake may be heterogeneous among β cells, and the degree of glucose uptake may be related to both UPR activation and proliferation.

The work presented here suggests a possible approach to therapeutic expansion of β cell mass. However, β cells are sensitive to ER stress, which when unresolved is a primary cause of β cell loss in both autoimmune and obesity-related diabetes (3, 4, 6, 63–65). Placing UPR as the sensor of insulin demand that determines β cell number offers one explanation for this heightened susceptibility. Potential therapies utilizing UPR to promote β cell proliferation would have to take into consideration the current level of β cell stress and operate within a narrow safety window to avoid overload and cell death. It remains to be determined how the glucose dependence of UPR-induced proliferation observed in vitro translates to the in vivo condition. This work also raises the possibility that agents that reduce β cell stress from the decompensated range to the adaptive range might have the potential to reset the stress rheostat to enable mild stress to expand β cell mass. Tools are needed to measure, and to modulate, β cell stress level in vivo.

Translating mouse β cell findings to human tissue has been challenging (40, 41). Human β cells have lower basal proliferation than mouse and respond less well to stimulation (40, 41). Furthermore, islets from people with diabetes show evidence of decompensated ER stress (31, 64). Our finding that human β cells from most, but not all, donors proliferated in response to UPR offers a potential handle to move toward identifying the genetic, epigenetic, and acquired factors that impact human β cell mass accrual in response to insulin demand. UPR pathway activation is influenced by genetics in mice (29). Combined with means of measuring and modulating in vivo β cell stress, this knowledge may allow patient-specific therapies to enhance β cell mass.

Remaining areas of uncertainty include the nature of the precise signal that activates UPR, whether the adaptive proliferative response can be sustained under chronic ER stress conditions, and whether this is due to ER peptide load from proinsulin synthesis, ER redox status, calcium handling, or other insult. A role for ATF6 in demand-driven β cell mass in vivo has not yet been demonstrated. ATF6 targets that drive proliferation remain to be discovered. However, the current work represents an important step forward in understanding how β cell number adapts to insulin demand, and it may illustrate a new paradigm linking organ size to physiological need.

Methods

Mice. Glucose infusions were performed as described (15); 10- to 12-week-old C57BL/6J male mice received continuous i.v. infusions of saline (in the femoral vein for those performed at University of Pittsburgh School of Medicine, and in the jugular vein for those performed at UMass Medical School) or 50% dextrose for 4 days. They then were euthanized for islet isolation or pancreas histology. High-fat feeding was performed as described (28); 10- to 12-week-old C57BL/6J male mice were fed control chow or 60% lard diet (catalog TD.06414, Harlan) for 7 days. INS2(C96YAkita) mice or *db/db*-C57BLKS mice (both from The Jackson Laboratory) were studied, with littermate controls.

Males and females showed similar results and were combined. For TUDCA experiments, mice were injected i.p. with 500 μg/kg TUDCA or saline (HFD-fed mice) or PBS (Akita and *db/db* mice) twice daily for 2 days prior to sacrifice. To measure proliferation, for HFD, mice received 40 mg/kg BrdU i.p. twice daily (am and pm) for 2 days with the TUDCA injections. Akita and *db/db* mice received 2 injections of 40 mg/kg BrdU at 4 hours and 2 hours prior to euthanasia. Two hours after the final injection, mice were euthanized and pancreata processed for histology. Blood glucose measurements were completed by AlphaTRAK glucometer (Abbott).

Mouse islet isolation, dispersion, and culture. Islets were isolated as described (24), by collagenase digestion and ficoll-hypaque density gradient separation. For all primary islet cell experiments, islets were cultured overnight in islet complete media (ICM, RPMI containing 10% FBS, penicillin/streptomycin, and 5 mM glucose). The following day, islets were hand-picked and trypsinized (0.05% trypsin), and single cells were plated on uncoated coverslips for immunofluorescence or on uncoated plastic for Western blots and RNA. To minimize variability, dispersed-islet proliferation assays, FBS from a single vendor (Atlantic Biologicals), and lot was used; islet culture medium was mixed in bulk and stockpiled in small volumes; and trypsin for islet dispersion was frozen in single-use tubes. Controls were performed on each biological replicate to minimize impact of variability on experimental result. When an experiment required more islets than were obtainable from one mouse, islets from multiple mice were pooled to achieve one biological replicate. Treatments were administered for 72 hours for immunoblots and immunostaining (final 24 hours with BrdU), or 6, 24, or 48 hours for quantitative PCR (qPCR).

Proteomics screen. C57BL/6J 10- to 12-week-old male mice were infused for 4 days with saline or glucose, as above. Pancreatic islets were isolated and hand-picked on ice in ICM containing 1% FBS. Islet lysates from 4 mice in each condition were pooled, labeled with Cy3 or Cy5 (University of Pittsburgh Proteomics Core), combined, focused to 70,000 volt-hours (IPGphor power source, Bio-Rad) on Immobiline pH 4-10 isoelectric focusing strips, and separated by SDS-PAGE (66). Gel images (Typhoon scanner, GE Healthcare) were visually evaluated for spot intensity change. Gels were poststained with Coomassie (Bio-Rad) and 24 proteins of interest were manually excised (OneTouch, The Gel Co.). Following trypsin digestion (Trypsin Gold, Promega), peptides were eluted, dehydrated, dissolved in 50% acetonitrile/0.3% trifluoroacetic acid/1 mM citric acid with an equal volume of saturated α-cyano-4-hydroxy cinnamic acid, and spotted on a MALDI plate (Applied Biosystems). MALDI-TOF analysis, performed on an ABI 4700 Mass Spectrometer at the University of Pittsburgh Integrated Core Facility, identified 18 unique proteins (Supplemental Table 1).

Immunoblots. Islet cells were washed with PBS and lysed in 125 mmol/l tris, 2% SDS, 1 mmol/l dithiothreitol, 20 μg/ml 4-aminophenylmethanesulfonyl fluoride hydrochloride (APMSF), and protease inhibitors, directly added to the culture well. Cells were detached from the plastic with a cut pipette tip, and samples were sonicated for 10 minutes with 30-second pulses and 30-second rests at 4 degrees. Samples were boiled in SDS-PAGE loading buffer for 5–10 minutes. After separation on SDS-PAGE, proteins were transferred to PVDF membrane, and the membrane was then blocked for 1–2 hours with 5% skim milk powder containing PBS and 0.1% Tween-20. Membranes were probed with antibodies from Abcam (p-IRE1, catalog ab124945), BD Biosciences (BiP, catalog 610978), Cell Signaling Technology (sXBP, catalog 12782; CHOP, catalog 2895; activated caspase 3, catalog 9661; GRP94, catalog 2104; p-eIF2α, catalog 9721; PDI, catalog 2446; and IRE1, catalog 3294), EMD Millipore (actin, catalog MAB1501; Cre, catalog 69050), Imagenex (ATF6, catalog IMG-273), Novus Biologicals (ATF6, catalog NBP1-40256), Santa Cruz Biotechnology Inc. (PCNA, catalog sc-56), and Sigma-Aldrich (Flag, catalog F1804). Blots were developed using ECL, ECL prime (GE Healthcare) or SuperSignal West Femto Maximum Sensitivity Substrate (Thermo Scientific). Band intensity was quantified using ImageJ (NIH).

RNA isolation and qPCR. RNA was isolated from intact islets (in vivo glucose infusion) or dispersed islets (cell culture experiments) using an all-in-one RNA purification kit (Norgen Biotek Corp.). RNA quality and quantity were verified by RNA integrity number and Nanodrop. cDNA was synthesized from 100–500 ng total RNA using iScript cDNA synthesis kit (Bio-Rad). qPCR was performed using SYBR green detection on RealPlex 2 and 4 cyclers (Eppendorf). For the semi-quantitative gel-based assay for Xbp splicing, cDNA amplified at 98°C for 2 minutes, 29 cycles of 98°C for 30 seconds, 60°C for 30 seconds, 72°C for 30 seconds, and final extension at 72°C for 5 minutes was run on a 2% agarose gel and imaged using a GelDoc (UVP LLC.). Primers were obtained from the literature (Supplemental Table 4). Data are expressed as ddCt (fold change). For *XBP1* splicing, semi-qPCR was followed by agarose electrophoresis; bands were quantified using ImageJ (NIH).

Flow cytometry. After culture treatments, dispersed islet cells were detached from the plate using trypsin. Cells in suspension were either not fixed (for Annexin V/PI staining) or fixed with 4% PFA for 20 minutes on ice. Cells were then washed twice with ice-cold PBS and left at 4 degrees until staining. On the day of staining, cells in PBS were centrifuged and fixed again for 5 minutes on ice with BD cytofix/cytoperm buffer (BD Biosciences). After washing, cells were resuspended in DPBS containing 300 μg/ml DNase for DNA digestion for BrdU staining. Cells were incubated at 37°C for 1 hour and then washed with BD perm/wash buffer (BD Biosciences). Staining was performed using anti–insulin-488 antibody (Cell Signaling Technology), BrdU-PE (BioLegend), and unconjugated mouse-BiP antibody for 20–30 minutes on ice. After washing, anti-mouse APC-labeled antibody was added for 20–30 minutes. For culture cell counts, samples were prepared as above, without DNAse, and with an additional label using mouse anti-glucagon conjugated to Zenon Pacific Blue (Invitrogen). Cells were counted at the same speed for a fixed time for each sample to assess relative cell number. Experiments were analyzed using an LSRII flow cytometer (BD Biosciences) and FlowJo software. Annexin V/PI staining was performed according to the manufacturer's protocol (Millipore), with analysis using a BD Accuri C6 flow cytometer (BD Biosciences) and Flowjo software.

IHC and immunocytochemistry. Pancreas and gut were fixed with 4% formalin (v/v) at room temperature for 5 hours and embedded in paraffin. Five to 7 micron sections were blocked and labeled using primary antibodies listed below and with DyLight secondary antibodies (Jackson ImmunoResearch Laboratories Inc.). For immunocytochemistry, dispersed islet cells were fixed with 4% paraformaldehyde for 10 minutes at room temperature. For BrdU staining, slides or coverslips were preincubated in 1N HCl for 30 minutes at 37°C prior to block step. Antibodies used for immunostaining were from Abcam (BrdU, catalog ab6326; insulin, catalog ab7842), BD Biosciences (BiP, catalog 610978), Cell Signaling Technology (γ-H2AX, cat-

alog 9718; pHH3, catalog 3377), and Santa Cruz Biotechnology Inc. (PCNA, catalog sc-56). Images were acquired using a Nikon florescent microscope, blinded, and manually counted. For transmission electron microscopy, pancreas was fixed in 2.5% glutaraldehyde/2% paraformaldehyde and postfixed in aqueous 1% OsO_4, 1% $K_3Fe(CN)_6$. After dehydration through a graded ethanol series, samples were infiltrated in a 1:1 mixture of propylene oxide/Polybed 812 epoxy resin (Polysciences Inc.), embedded, cured at 37°C overnight, and hardened at 65°C for 2 more days. Ultrathin (70 nm) sections were collected on 200 mesh copper grids and stained with 2% uranyl acetate in 50% methanol for 10 minutes, followed by 1% lead citrate for 7 minutes. Sections were imaged using a JEOL JEM 1011 transmission electron microscope at 80 kV fitted with a side mount AMT digital camera (Advanced Microscopy Techniques).

Transfection and adenoviral infection. Plasmids were obtained from Addgene (ATF6α, IRE1α, and sXbp) or OriGene (sh-ATF6 and sh-IRE1). Islets were dispersed to single cells and washed with PBS. Plasmid was added, and cells were electroporated at 950 mV with 2 shocks of 20 ms using the Neon transfection system (Invitrogen). Viability before and after electroporation (Supplemental Figure 12) was measured by adding 1 μl of TO-PRO-3 (Invitrogen) to cells suspended in 100 μl of PBS, followed by flow cytometry on a BD LSRII and analysis using FlowJo software. Dispersed transfected cells were plated on plastic for Western blot or on coverslips for immunocytochemistry, where they were allowed 24 hours to recover prior to treatment. Adenovirus expressing mouse Cyclin D2 or control (Vector BioLabs) was used at 10 MOI to transduce dispersed islet cells on the day after plating.

Human islet culture. Human islets received from Integrated Islet Distribution Program (IIDP) were allowed to recover in ICM for 24–48 hours. Islets were picked, dispersed, and plated on coverslips as above, except that treatments with glucose and drugs were for 96 hours, with BrdU added at the start of the treatment. The percent of β cells of human islet preparations was determined by dividing the total number of nuclei, as determined by DAPI staining, by the number of insulin-stained cells, in the control 7.5 mM glucose condition using images obtained for the experiment shown in Figure 9A. Adenovirus expressing human ATF6 or control (Vector BioLabs) was used at 10 MOI to transduce dispersed human islet cells the day after plating. After 96 hours, cells were fixed and stained as above.

Chemicals. Chemicals used included Tg (doses per text), TUDCA (100 ng/ml), PBA (250 nM), and Brdu (40 mg/kg) (all from Sigma-Aldrich), along with Tm (doses per text), ATF6 inhibitor AEBSF (100 nM), PERK inhibitor GSK2606414 (5 nM), and IRE1 inhibitor 4μ8c (7 μM) (all from EMD).

Statistics. Data are represented as mean ± SEM of *n* independent mice or independent islet preparations. Statistical analyses were performed using Prism (GraphPad). *P* values are calculated by 2-tailed Student's *t* test or 1-way ANOVA with Sidak post-test for multiple comparisons; $P < 0.05$ was considered significant.

Study approval. Mice were maintained at UMass Medical School or the University of Pittsburgh. All procedures were approved by their respective Institutional Care and Use Committees.

Acknowledgments

Human pancreatic islets were provided by the NIDDK-funded IIDP at City of Hope. We thank the University of Pittsburgh Proteomics Core, Integrated Core Facility, and Donna Stolz at the Center for Biological Imaging for assistance with the proteomics screen and electron microscopy, respectively, and the National Mouse Metabolic Phenotyping Center at UMass Medical School, supported by U24-DK093000, to Jason Kim. This study was funded by the NIH: DK076562 (to L.C. Alonso), DK095140 (to L.C. Alonso), and DK48280 (to P. Arvan). We are also grateful for many important discussions with our friends and colleagues and the Beta Cell Group at UMass.

Address correspondence to: Laura C. Alonso, Diabetes Division, UMass Medical School, 368 Plantation Street, Worcester, Massachusetts 01605, USA. Phone: 774.455.3640; E-mail: Laura.Alonso@umassmed.edu.

1. Weir GC, Bonner-Weir S. Islet β cell mass in diabetes and how it relates to function, birth, and death. *Ann N Y Acad Sci*. 2013;1281:92–105.
2. Costes S, Langen R, Gurlo T, Matveyenko AV, Butler PC. β-Cell failure in type 2 diabetes: a case of asking too much of too few? *Diabetes*. 2013;62(2):327–335.
3. Back SH, Kaufman RJ. Endoplasmic reticulum stress and type 2 diabetes. *Annu Rev Biochem*. 2012;81:767–793.
4. Papa FR. Endoplasmic reticulum stress, pancreatic β-cell degeneration, and diabetes. *Cold Spring Harb Perspect Med*. 2012;2(9):a007666.
5. Mirmira RG. Saturated free fatty acids: islet β cell "stressERs". *Endocrine*. 2012;42(1):1–2.
6. Eizirik DL, Cnop M. ER stress in pancreatic beta cells: the thin red line between adaptation and failure. *Sci Signal*. 2010;3(110):pe7.
7. Ron D, Harding HP. Protein-folding homeostasis in the endoplasmic reticulum and nutritional regulation. *Cold Spring Harb Perspect Biol*. 2012;4(12):a013177.
8. Sachdeva MM, Stoffers DA. Minireview: Meeting the demand for insulin: molecular mechanisms of adaptive postnatal beta-cell mass expansion. *Mol Endocrinol*. 2009;23(6):747–758.
9. Butler AE, et al. Hematopoietic stem cells derived from adult donors are not a source of pancreatic β-cells in adult nondiabetic humans. *Diabetes*. 2007;56(7):1810–1816.
10. Dor Y, Brown J, Martinez OI, Melton DA. Adult pancreatic β-cells are formed by self-duplication rather than stem-cell differentiation. *Nature*. 2004;429(6987):41–46.
11. Georgia S, Bhushan A. Beta cell replication is the primary mechanism for maintaining postnatal β cell mass. *J Clin Invest*. 2004;114(7):963–968.
12. Teta M, Rankin MM, Long SY, Stein GM, Kushner JA. Growth and regeneration of adult β cells does not involve specialized progenitors. *Dev Cell*. 2007;12(5):817–826.
13. Brennand K, Huangfu D, Melton D. All β cells contribute equally to islet growth and maintenance. *PLoS Biol*. 2007;5(7):e163.
14. Fontés G, et al. Glucolipotoxicity age-dependently impairs beta cell function in rats despite a marked increase in β cell mass. *Diabetologia*. 2010;53(11):2369–2379.
15. Alonso LC, et al. Glucose infusion in mice: a new model to induce β-cell replication. *Diabetes*. 2007;56(7):1792–1801.
16. Bonner-Weir S, Deery D, Leahy JL, Weir GC. Compensatory growth of pancreatic β-cells in adult rats after short-term glucose infusion. *Diabetes*. 1989;38(1):49–53.
17. Flier SN, Kulkarni RN, Kahn CR. Evidence for a circulating islet cell growth factor in insulin-resistant states. *Proc Natl Acad Sci U S A*. 2001;98(13):7475–7480.
18. Salpeter SJ, Khalaileh A, Weinberg-Corem N, Ziv O, Glaser B, Dor Y. Systemic regulation of the age-related decline of pancreatic β-cell replication. *Diabetes*. 2013;62(8):2843–2848.
19. Porat S, et al. Control of pancreatic β cell regeneration by glucose metabolism. *Cell Metab*. 2011;13(4):440–449.
20. Metukuri MR, et al. ChREBP mediates glucose-stimulated pancreatic β-cell proliferation. *Diabetes*. 2012;61(8):2004–2015.
21. El Ouaamari A, et al. Liver-derived systemic factors drive βcell hyperplasia in insulin-resistant states. *Cell Rep*. 2013;3(2):401–410.

22. Demirci C, et al. Loss of HGF/c-Met signaling in pancreatic β-cells leads to incomplete maternal β-cell adaptation and gestational diabetes mellitus. *Diabetes*. 2012;61(5):1143–1152.
23. Zarrouki B, et al. Epidermal growth factor receptor signaling promotes pancreatic β-cell proliferation in response to nutrient excess in rats through mTOR and FOXM1. *Diabetes*. 2014;63(3):982–993.
24. Pascoe J, et al. Free fatty acids block glucose-induced β-cell proliferation in mice by inducing cell cycle inhibitors p16 and p18. *Diabetes*. 2012;61(3):632–641.
25. Yokoe T, et al. Intermittent hypoxia reverses the diurnal glucose rhythm and causes pancreatic β-cell replication in mice. *J Physiol*. 2008;586(3):899–911.
26. Chang SC, et al. Rat gene encoding the 78-kDa glucose-regulated protein GRP78: its regulatory sequences and the effect of protein glycosylation on its expression. *Proc Natl Acad Sci U S A*. 1987;84(3):680–684.
27. Hetz C, et al. The disulfide isomerase Grp58 is a protective factor against prion neurotoxicity. *J Neurosci*. 2005;25(11):2793–2802.
28. Stamateris RE, Sharma RB, Hollern DA, Alonso LC. Adaptive β-cell proliferation increases early in high-fat feeding in mice, concurrent with metabolic changes, with induction of islet cyclin D2 expression. *Am J Physiol Endocrinol Metab*. 2013;305(1):E149–E159.
29. Chan JY, Luzuriaga J, Bensellam M, Biden TJ, Laybutt DR. Failure of the adaptive unfolded protein response in islets of obese mice is linked with abnormalities in β-cell gene expression and progression to diabetes. *Diabetes*. 2013;62(5):1557–1568.
30. Song B, Scheuner D, Ron D, Pennathur S, Kaufman RJ. Chop deletion reduces oxidative stress, improves beta cell function, and promotes cell survival in multiple mouse models of diabetes. *J Clin Invest*. 2008;118(10):3378–3389.
31. Laybutt DR, et al. Endoplasmic reticulum stress contributes to beta cell apoptosis in type 2 diabetes. *Diabetologia*. 2007;50(4):752–763.
32. Matsuda T, et al. Ablation of C/EBPβ alleviates ER stress and pancreatic β cell failure through the GRP78 chaperone in mice. *J Clin Invest*. 2010;120(1):115–126.
33. Oyadomari S, et al. Targeted disruption of the Chop gene delays endoplasmic reticulum stress-mediated diabetes. *J Clin Invest*. 2002;109(4):525–532.
34. Yoshioka M, Kayo T, Ikeda T, Koizuni A. A novel locus, Mody4, distal to D7Mit189 on chromosome 7 determines early-onset NIDDM in nonobese C57BL/6 (Akita) mutant mice. *Diabetes*. 1997;46(5):887–894.
35. Kayo T, Koizumi A. Mapping of murine diabetogenic gene mody on chromosome 7 at D7Mit258 and its involvement in pancreatic islet and β cell development during the perinatal period. *J Clin Invest*. 1998;101(10):2112–2118.
36. Özcan U, et al. Chemical chaperones reduce ER stress and restore glucose homeostasis in a mouse model of type 2 diabetes. *Science*. 2006;313(5790):1137–1140.
37. Axten JM, et al. Discovery of 7-methyl-5-(1-{[3-(trifluoromethyl)phenyl]acetyl}-2,3-dihydro-1H-indol-5-yl)-7H-pyrrolo[2,3-d]pyrimidin-4-amine (GSK2606414), a potent and selective first-in-class inhibitor of protein kinase R (PKR)-like endoplasmic reticulum kinase (PERK). *J Med Chem*. 2012;55(16):7193–7207.
38. Cross BC, et al. The molecular basis for selective inhibition of unconventional mRNA splicing by an IRE1-binding small molecule. *Proc Natl Acad Sci U S A*. 2012;109(15):E869–E878.
39. Okada T, et al. A serine protease inhibitor prevents endoplasmic reticulum stress-induced cleavage but not transport of the membrane-bound transcription factor ATF6. *J Biol Chem*. 2003;278(33):31024–31032.
40. Bernal-Mizrachi E, et al. Human β-cell proliferation and intracellular signaling part 2: still driving in the dark without a road map. *Diabetes*. 2014;63(3):819–831.
41. Kulkarni RN, Mizrachi EB, Ocana AG, Stewart AF. Human β-cell proliferation and intracellular signaling: driving in the dark without a road map. *Diabetes*. 2012;61(9):2205–2213.
42. Luo B, Lee AS. The critical roles of endoplasmic reticulum chaperones and unfolded protein response in tumorigenesis and anticancer therapies. *Oncogene*. 2013;32(7):805–818.
43. Scheuner D, et al. Control of mRNA translation preserves endoplasmic reticulum function in β cells and maintains glucose homeostasis. *Nat Med*. 2005;11(7):757–764.
44. Longuet C, et al. Liver-specific disruption of the murine glucagon receptor produces α-cell hyperplasia: evidence for a circulating α-cell growth factor. *Diabetes*. 2013;62(4):1196–1205.
45. Fukagawa M, Nakanishi S, Kazama JJ. Basic and clinical aspects of parathyroid hyperplasia in chronic kidney disease. *Kidney Int Suppl*. 2006;(102):S3–S7.
46. Mittag J, Friedrichsen S, Strube A, Heuer H, Bauer K. Analysis of hypertrophic thyrotrophs in pituitaries of athyroid $Pax8^{-/-}$ mice. *Endocrinology*. 2009;150(9):4443–4449.
47. Horvath E, Kovacs K, Scheithauer BW. Pituitary hyperplasia. *Pituitary*. 1999;1(3–4):169–179.
48. Barber TM, Adams E, Ansorge O, Byrne JV, Karavitaki N, Wass JA. Nelson's syndrome. *Eur J Endocrinol*. 2010;163(4):495–507.
49. Hodish I, et al. In vivo misfolding of proinsulin below the threshold of frank diabetes. *Diabetes*. 2011;60(8):2092–2101.
50. Matveyenko AV, Gurlo T, Daval M, Butler AE, Butler PC. Successful versus failed adaptation to high-fat diet-induced insulin resistance: the role of IAPP-induced β-cell endoplasmic reticulum stress. *Diabetes*. 2009;58(4):906–916.
51. Cunha DA, et al. Death protein 5 and p53-upregulated modulator of apoptosis mediate the endoplasmic reticulum stress-mitochondrial dialog triggering lipotoxic rodent and human β-cell apoptosis. *Diabetes*. 2012;61(11):2763–2775.
52. Wang R, Munoz EE, Zhu S, McGrath BC, Cavener DR. Perk gene dosage regulates glucose homeostasis by modulating pancreatic β-cell functions. *PLoS One*. 2014;9(6):e99684.
53. Gao Y, et al. PERK is required in the adult pancreas and is essential for maintenance of glucose homeostasis. *Mol Cell Biol*. 2012;32(24):5129–5139.
54. Lee AH, Heidtman K, Hotamisligil GS, Glimcher LH. Dual and opposing roles of the unfolded protein response regulated by IRE1α and XBP1 in proinsulin processing and insulin secretion. *Proc Natl Acad Sci U S A*. 2011;108(21):8885–8890.
55. Thorpe JA, Schwarze SR. IRE1α controls cyclin A1 expression and promotes cell proliferation through XBP-1. *Cell Stress Chaperones*. 2010;15(5):497–508.
56. Usui M, et al. Atf6α-null mice are glucose intolerant due to pancreatic β-cell failure on a high-fat diet but partially resistant to diet-induced insulin resistance. *Metabolism*. 2012;61(8):1118–1128.
57. Engin F, et al. Restoration of the unfolded protein response in pancreatic β cells protects mice against type 1 diabetes. *Sci Transl Med*. 2013;5(211):211ra156.
58. Elouil H, et al. Acute nutrient regulation of the unfolded protein response and integrated stress response in cultured rat pancreatic islets. *Diabetologia*. 2007;50(7):1442–1452.
59. Vander Mierde D, et al. Glucose activates a protein phosphatase-1-mediated signaling pathway to enhance overall translation in pancreatic β-cells. *Endocrinology*. 2007;148(2):609–617.
60. Greenman IC, Gomez E, Moore CE, Herbert TP. Distinct glucose-dependent stress responses revealed by translational profiling in pancreatic β-cells. *J Endocrinol*. 2007;192(1):179–187.
61. Sidrauski C, McGeachy AM, Ingolia NT, Walter P. The small molecule ISRIB reverses the effects of eIF2α phosphorylation on translation and stress granule assembly. *eLife*. 2015;4:e05033.
62. Blandino-Rosano M, et al. mTORC1 signaling and regulation of pancreatic β-cell mass. *Cell Cycle*. 2012;11(10):1892–1902.
63. Tersey SA, et al. Islet β-cell endoplasmic reticulum stress precedes the onset of type 1 diabetes in the nonobese diabetic mouse model. *Diabetes*. 2012;61(4):818–827.
64. Marhfour I, et al. Expression of endoplasmic reticulum stress markers in the islets of patients with type 1 diabetes. *Diabetologia*. 2012;55(9):2417–2420.
65. Yang C, Diiorio P, Jurczyk A, O'Sullivan-Murphy B, Urano F, Bortell R. Pathological endoplasmic reticulum stress mediated by the IRE1 pathway contributes to pre-insulitic beta cell apoptosis in a virus-induced rat model of type 1 diabetes. *Diabetologia*. 2013;56(12):2638–2646.
66. Unlü M, Morgan ME, Minden JS. Difference gel electrophoresis: a single gel method for detecting changes in protein extracts. *Electrophoresis*. 1997;18(11):2071–2077.